Chemical Science

ROYAL SOCIETY OF CHEMISTRY

REVIEW

View Article Online
View Journal | View Issue

Cite this: *Chem. Sci.*, 2022, **13**, 10985

Fluorine in metal-catalyzed asymmetric transformations: the lightest halogen causing a massive effect

Samuel Lauzon and Thierry Ollevier *

Received 21st February 2022
Accepted 6th August 2022

DOI: 10.1039/d2sc01096h

rsc.li/chemical-science

This review aims at providing an overview of the most significant applications of fluorine-containing ligands reported in the literature starting from 2001 until mid-2021. The ligands are classified according to the nature of the donor atoms involved. This review highlights both metal–ligand interactions and the structure–reactivity relationships resulting from the presence of the fluorine atom or fluorine-containing substituents on chiral catalysts.

1. Introduction

Fluoroorganic molecules have received widespread interest in recent research in view of the fact that their synthesis is virtually missing from any biological processes. Being the 13th most abundant element in the lithosphere, fluorine is mostly present in water-insoluble minerals, *i.e.*, fluorspar (CaF_2), cryolite (Na_3AlF_6), and fluoroapatite ($Ca_5(PO_4)_3F$), which limits its uptake into living organisms.[1] Also, the nucleophilicity of fluoride is diminished by its high hydration energy, and therefore, this anion is inadequate for any nucleophilic substitution reactions in aqueous media. As a result, only a dozen of naturally occurring fluorometabolites, *i.e.*, fluoroacetic acid, ω-fluorinated fatty acids, (2*R*,3*R*)-2-fluorocitric acid, (2*S*,3*S*,4*R*,5*R*)-nucleocidin, and (2*S*,3*S*)-4-fluorothreonine, have been identified so far.[2] Since then, such scarcity has been compensated for by man-made fluorine-containing pharmaceuticals, of which many have been welcomed as blockbuster drugs on the market.[3] Molecular conformation, membrane permeability, and metabolic stability are all properties affected by fluorine substitution, but the impact on the pharmacodynamics and pharmacokinetics of a lead remains quite unpredictable.[4] The

Département de Chimie, Université Laval, 1045 Avenue de la Médecine, Québec, QC G1V 0A6, Canada. E-mail: thierry.ollevier@chm.ulaval.ca

Samuel Lauzon was born in Québec, Canada. He joined the research group of Professor Thierry Ollevier as an undergraduate intern student in 2015. He obtained his MSc in 2018 working on asymmetric iron catalysis. He received his PhD in organic chemistry at Université Laval (Québec, Canada) under the supervision of Professor Thierry Ollevier in 2022. His work involved the development of designer 2,2′-bipyridinediol ligands for applications in metal-catalyzed asymmetric transformations. He is currently interested in ligand design, crystallization of chiral catalysts, transition state models, and environmentally benign catalysis.

Thierry Ollevier was born in Brussels and obtained his Licence (1991) and PhD (1997) at the University of Namur (Belgium) and was a post doctorate fellow at the Université catholique de Louvain (Belgium), under István E. Markó (1997), a NATO and BAEF post-doctorate fellow at Stanford University under Barry M. Trost (1998–2000), and then a post doctorate fellow at the Université de Montréal under André B. Charette (2000–2001). After an Assistant Professor appointment (2001) at Université Laval (Québec, Canada), he became Associate (2006) and is currently Full Professor. Current research in his group aims at designing novel catalysts, developing catalytic reactions and applying these methods to chemical synthesis. He is active in the areas of asymmetric catalysis, iron catalysis, diazo chemistry, fluorine chemistry, and flow chemistry. He has served as a member of the Advisory Board of SynOpen since 2019, as an Associate Editor of RSC Advances since 2015 and was admitted as a Fellow of the Royal Society of Chemistry (2016).

Table 1 Electronegativities of selected atoms and functional groups

Atom or group	χ_P	χ_e	χ_H	χ_J
H	2.20	2.28	—	—
F	3.98	3.95	—	—
Cl	3.16	3.03	—	—
Br	2.96	2.80	—	—
I	2.66	2.47	—	—
NO_2	—	3.40	—	—
CN	—	3.30	—	—
CF_3	—	3.35	3.46	3.29
CHF_2	—	—	3.00	2.94
CH_2F	—	—	2.61	2.61
CH_3	—	2.30	2.27	2.30

specific behaviour of fluorinated compounds arises from the short, strong, and highly polarized C–F bond that electrostatically pairs with the neighbouring atoms, bonds, and lone pairs.[5] Instead of being targeted only for biological activity purposes, various chiral organofluorine compounds were employed as catalysts in asymmetric transformations.[6] Among the known strategies for designing enhanced stereodiscriminating catalysts,[7] the conversion of known catalytic systems into F-containing ones unlocked new interesting features ensuing from the fluorine effect. Chiral fluorinated catalysts benefit from (i) electronically and (ii) sterically customized properties and (iii) being used in fluorous biphasic systems (FBS). Since an increased reactivity in acid catalysts is often a synonym of electronic deficiency, Pauling (χ_P), empirical (χ_e), Huheey (χ_H), and Jaffé (χ_J) electronegativities values are provided for a selection of atoms and groups (Table 1).[8] Fluorine is the most electronegative element on the Pauling scale ($\chi_P = 3.98$) and is most frequently used as an electronically impoverishing substituent in ligands. The CF_3 group is also electronically deficient, much more than other *C*-based substituents, and its χ value is similar to the ones of the CN and NO_2 groups, known as strongly electron withdrawing groups (EWG). A set of steric parameters, *e.g.*, *A* values ($-\Delta G$),[9] Taft ($-E_s$),[10] Charton (ν),[11] and biphenyl rotational interference values (I^{X-H}),[12] and Boltzmann-weighted Sterimol parameters (wB_1, wL, and wB_5),[13] eases the comparison of bulkiness between selected atoms and functional groups (Table 2). Fluorine is a small element (van der Waals radius = 1.47 Å *vs.* 1.20 Å for H *vs.* 1.52 Å for O)[14] and generally causes minimal steric perturbation upon H to F exchange, whereas the substitution of C–H by C–F in a methyl group successively leads to an increase in size (Me < CH_2F < CHF_2 < CF_3). Thus, fluorine is a powerful tool to increase the steric hindrance – even more in polyfluoroalkyl groups – rendering the CF_3 group as a bulky substituent in the general order Me < ^{i}Pr ~ CF_3 ≪ Ph ~ ^{t}Bu. The CF_3 group is a key component for fine-tuning simultaneously the steric and electronic properties, which is undeniably of great interest for ligand design. Following the "like dissolves like" principle, a chiral ligand bearing sufficiently long perfluoroalkyl chains, *i.e.,* ponytails (R_F), acquires a strong affinity for the fluorous phase, also called "fluorophilicity".[15] This engineered technology involves the temperature-dependent miscibility of fluorous-organic solvents leading to partition of two phases at lower temperature. The fluorous ligand (or catalyst) can be selectively separated from the reactant/product mixture and recovered using various experimental methods.

The synergistic participation of the steric, electronic, and physical properties brought up by the chiral fluorinated ligand may modulate the stereoselective event of a reaction positively *vs.* "fluorine-free transition states (TS)". This review highlights both metal–ligand interactions and structure–reactivity relationship related to the presence of the fluorine atom or fluorine-containing substituents on chiral catalysts. The article focusses on the molecular architecture of the ligands rather than on the type of reaction they were employed in. The selection of chiral fluoroorganic ligands are classified according to *O*-, *N*,*O*-, *N*-, *P*, *N*-, *P*- and *C*-binding modes with metals. The advantages of using catalytic systems involving fluorine for both the reactivity and the stereochemical outcomes are highlighted, compared,

Table 2 Steric parameters of selected atoms and functional groups

					*w*Sterimol		
Atom or group	$-\Delta G$ (kcal mol^{-1})	$-E_s$	ν	I^{X-H} (kJ mol^{-1})	wB_1 (Å)	wL (Å)	wB_5 (Å)
H	—	0.00	0.00	~4.0	—	—	—
F	0.15	0.46	0.27	19.2	1.52	3.12	2.03
Cl	0.43	0.97	0.55	38.1	1.80	3.99	2.03
Br	0.38	1.16	0.65	42.5	1.95	4.29	2.03
CN	0.17	0.51	—	25.6	—	—	—
NO_2	1.10	1.01/2.52[a]	—	32.4	—	—	—
Me	1.70	1.24	0.52	40.4	1.88	3.43	2.02
CH_2F	1.59	1.48	0.62	—	—	—	—
CHF_2	1.85	1.91	0.68	—	—	—	—
CF_3	2.10	2.40	0.91	50.6	1.87	3.75	2.60
^{i}Pr	2.15	1.71	0.76	52.6	1.91	4.56	3.17
$SiMe_3$	2.50	3.36	1.40	47.2	—	—	—
Ph	3.00	1.01/3.82[a]	1.66	33.1	1.70	6.80	3.15
^{t}Bu	~4.20	2.78	1.24	76.6	2.76	4.54	3.17

[a] Thickness/width values.

and discussed. Furthermore, the effects on the stereochemical outcome arising from using fluorinated ligands *vs.* non-fluorinated ones are often provided when both results were available in the literature. The set of examples for promoting the massive effect of fluorine in metal-catalyzed asymmetric catalysis is not exhaustive; hence fluorinated reactants, solvents, additives, and Brønsted acids-based catalysts are not reviewed herein.

2. Chiral fluoroorganometallic complexes

2.1 *O*-Based binding modes

2.1.1 Phosphoric acids. Chiral phosphoric acid (CPA) ligands (R_a)-**1–3** and (S_a)-**4** were obtained by the phosphorylation of fluorinated 1,1′-bi-2-naphthol (BINOL)-type ligands and were described as promising candidates for enantioselective applications (Fig. 1). As an example, the fluorination reaction of β-ketoesters **5–8** using the 3 : 1 (R_a)-**1**/$ScCl_3$ complex afforded the corresponding α-fluorinated products **9–12** with 78–84% ee (Scheme 1).[16] The importance of the eight fluorine atoms was demonstrated based on the low 11% ee obtained for (+)-**9** using the Sc^{III} salt of the non-fluorinated CPA. On the other hand, (R_a)-**2** [17] and (R_a)-**3** [18] were respectively employed with Cu^{I} salts in the synthesis of chiral polyfluoro *N*-containing compounds, albeit with modest ees.

In another application, cycloadducts (*S*,*R*,*R*)-**15** and *endo*-(*R*,*S*,*S*,*S*)-**16**, respectively obtained from the hetero-Diels–Alder (HDA) and the Diels–Alder (DA) reactions between dienophile **13** and cyclopentadiene **14**, were synthesized with excellent yields and stereoselectivities using the binary (S_a)-**4**/In^{III} catalytic system (Scheme 2).[19] In most cases, a higher chemoselectivity was noted for the HDA cycloadduct *vs.* the DA one. The stereoselective induction was explained by the important π, π interaction, arising from an electrostatic pairing between one electronically deficient pentafluorophenyl ring and diene **14**, together with highly sensitive *ortho* positions occupied by F atoms.

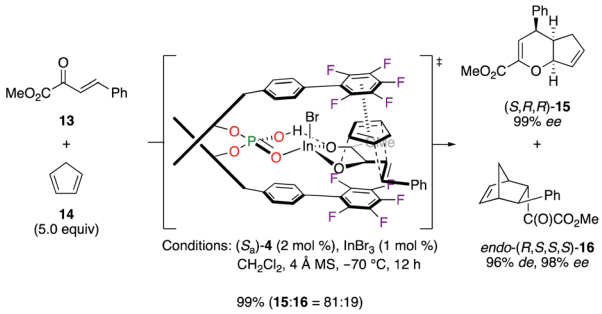

Scheme 2 (S_a)-**4**/In^{III}-catalyzed HDA and DA reactions.

2.1.2 Carboxylates and alkoxides. Known as valuable catalysts in the chemistry of diazo compounds, chiral Rh^{II} tetrakis(carboxylates) are rather expensive to be easily used in industrial applications. The recyclable chiral fluorous Rh^{II} complex (*S*)-**18** was then targeted in the cyclopropanation reaction of diazoester **19** and styrene **20** (Scheme 3).[20] Whereas it was less selective in terms of ee than (*S*)-**17**, the perfluoroalkyl chain allowed an efficient recovery of the catalyst using both liquid and solid fluorous phase extraction strategies. Slight improvements of the chiral induction were obtained in the insertion reaction of **19** into the C–H bond of cyclohexane using (*S*)-**18** under either homogeneous or heterogeneous conditions.

Various enantioselective organic transformations were performed using more sophisticated CF_3-containing BINOL-based chiral catalysts (Fig. 2). Indeed, the synergetic activation using self-assembled bifunctional chiral catalysis was shown as an efficient strategy in the hydrophosphonylation reaction of aldehydes.[21] The multiple reactive sites of catalyst (R_a)-**22**, generated *in situ* in the presence of $Ti(O^iPr)_4$, CF_3-aryl-substituted BINOL, and (−)-cinchonidine, allowed cooperative interactions between steric and electronic properties, as postulated in the transition state model of the reaction. Also,

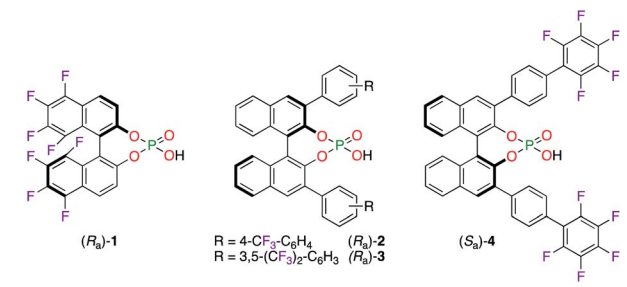

Fig. 1 Chiral fluorinated CPA ligands **1–4** in metal-catalyzed reactions.

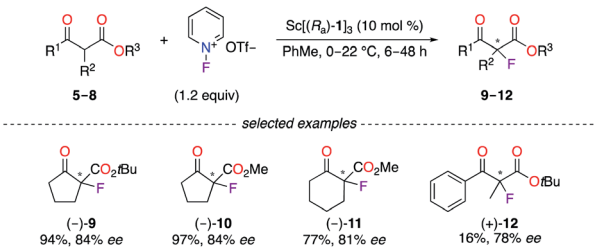

Scheme 1 [(R_a)-**1**]$_3$/Sc^{III}-catalyzed fluorination reaction.

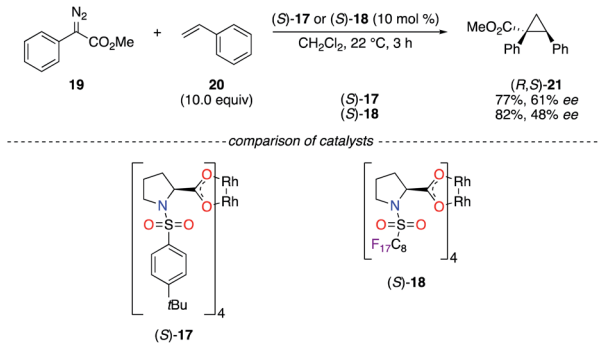

Scheme 3 Cyclopropanation reaction using chiral dirhodium catalysts.

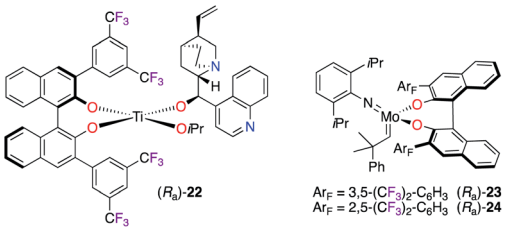

Fig. 2 Ti^{IV}– and Mo^{VI}–BINOLate complexes.

trifluoromethylated BINOLates showed excellent chiral induction in the desymmetrization of C_s-symmetric phosphaferrocenes *via* ring-closing metathesis using Mo^{VI}-catalysts (R_a)-**23** and (R_a)-**24**.[22]

2.1.3 Diols. Since hydrobenzoin **25** is cheap and readily available in its *R*,*R* and *S*,*S* enantiomeric forms, chiral Ti^{IV} complexes have employed the 1,2-diphenylethane-1,2-diol scaffold in the enantioselective oxidation reaction of 4-methylthioanisole **30** using cumyl hydrogen peroxide (CHP) as the oxidant (Scheme 4, conditions A).[23] The incorporation of OMe and CF_3 groups onto the chiral backbone of (*R*,*R*)-**26** and (*R*,*R*)-**27** led to electronically modified Ti^{IV} catalysts of lower capacity for chiral induction. As observed experimentally, a reversal of the asymmetric induction was observed using the 4-CF_3-C_6H_4 group (26% ee for (*R*)-**36**) *vs.* the unsubstituted one (80% ee for (*S*)-**36**), resulting in optically active sulfoxides of opposite signs. As postulated, competing mechanisms, arising from divergent binding modes with the Ti^{IV} centre, led to a decreased purity of **31** as the *S* enantiomer and to a complete reversal of the sense of chiral induction in favour of (*R*)-**31**. The Ti^{IV}-catalyzed asymmetric oxidation of aromatic sulfides was also demonstrated using a BINOL ligand comprising fluorine atoms at the 5, 5′, 6, 6′, 7, 7′, 8, and 8′ positions (Scheme 4, conditions B).[24] The oxidation of **30** by the (R_a)-**28**/Ti^{IV} system afforded (*R*)-**31** with

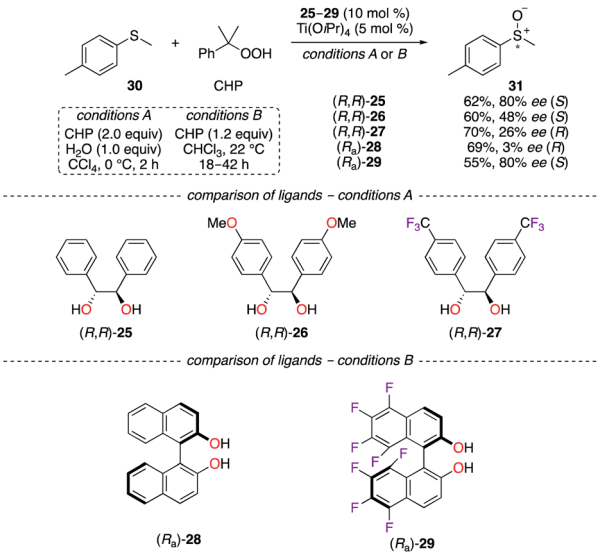

Scheme 4 Ti^{IV}-Catalyzed sulfoxidation reaction – (*R*,*R*)-hydrobenzoin and (R_a)-BINOL derivatives.

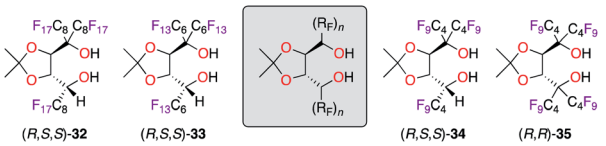

Fig. 3 TADDOL-like fluorous ligands.

virtually no enantioselectivity. Again, a reversal of the chiral induction was observed when (R_a)-**29** was employed and sulfoxide **31** was obtained as the *S* enantiomer in 80% ee. In the case of F_8BINOL (R_a)-**29**, the tenfold increase in acidity of the hydroxyl groups ($pK_a = 9.28$ *vs.* 10.28 for (R_a)-**28**) and the more positive oxidation potential ($E_2 = 2.07$ V *vs.* 1.47 V for (R_a)-**28**) are believed to result in a more configurationally stable chiral environment of the Ti^{IV}-based catalyst.

Being recognized along with BINOL as "privileged ligands",[25] α,α,α′,α′-tetraaryl-1,3-dioxolane-4,5-dimethanol (TADDOL) ligands have inspired the design of ligands **32–35**, bearing α,α,α′-triperfluoroalkyl and α,α,α′,α′-tetraperfluorobutyl chains (Fig. 3).[26] Being successfully employed in the Ti(^{i}PrO)$_4$-catalyzed methylation of various aldehydes, ligands (*R*,*S*,*S*)-**32–34** afforded similar levels of chiral induction (*ca.* 95% ee) in the benchmark reaction using benzaldehyde. Notably, shortening the fluorinated ponytails had no effect on the efficiency of the catalyst (C_4F_9 *vs.* C_8F_{17}), but the recyclability of the ligand was reduced; hence the use of an expensive fluorous solvent was therefore needed for extraction. Interestingly, only the tetrakis(perfluoroalkyl) analogue (*R*,*R*)-**35** was obtained from (*R*,*S*,*S*)-**34**, whereas the incorporation of a fourth perfluoroalkyl chain failed for diol (*R*,*S*,*S*)-**32** and (*R*,*S*,*S*)-**33** due to higher steric congestion. However, the (*R*,*R*)-**35**/Ti^{IV} catalyst was noticed to be inactive in the tested catalytic application.

BINOLs (R_a)-**36** and (S_a)-**37** were subjected to comparison studies in the addition of diphenylzinc to (*E*)-cinnamaldehyde **38** (Scheme 5).[27] As can be seen in (S_a)-**37**, the fluorine atoms increase the Lewis acidity of the Zn^{II} chelated metal centre. The higher enantioselectivity observed for (*R*)-**39** was then attributed to a better activation of the aldehyde by a more active catalyst,

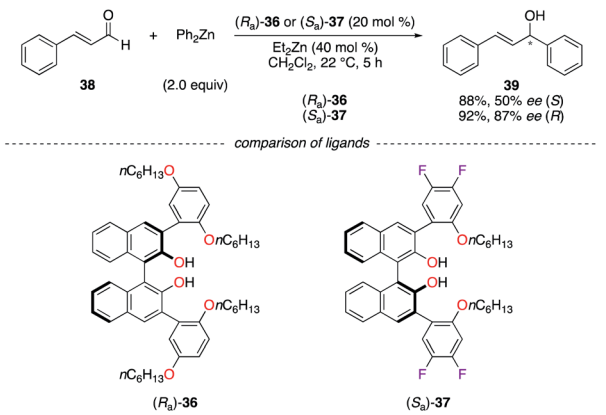

Scheme 5 Alkylation addition reaction of Ph_2Zn to cinnamaldehyde – (R_a)-**36** *vs.* (S_a)-**37**.

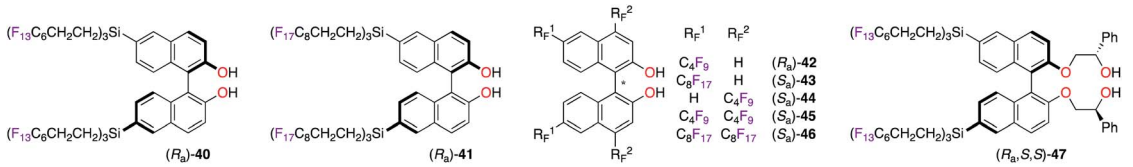

Fig. 4 Chiral R_F–BINOL ligands for Ti^{IV}-catalyzed reactions in FBS.

which favours the ligand-controlled pathway *vs.* the uncatalyzed background reaction.

Enantioselective applications in fluorous biphasic systems (FBS) were described for perfluorobutyl, -hexyl, and -octyl BINOL derivatives, *i.e.*, (R_a)-**40–42**,[28] (S_a)-**43–46**,[28c,29] and (R_a,*S*,*S*)-**47** (Fig. 4).[30] As an example, the addition of diethylzinc to a solution containing aldehydes **48–52** (0.20 equiv. each, total = 1.0 equiv.) in α,α,α-trifluorotoluene was performed using (R_a)-**40** (Scheme 6).[28a] All five aldehydes simultaneously reacted with the nucleophile under the optimal reaction conditions. Elution of the reaction mixture with acetonitrile, using fluorous reverse phase (FRP) silica gel chromatography, afforded alcohols (*R*)-**53–57** with ees up to 84%. The recovery of (R_a)-**40** from the fluorous phase was achieved using tetradecafluorohexane (FC-72) as the eluent. Also, a recycling protocol using a fluorous biphasic system based on (perfluoro)methyldecalin was suitable to recover (S_a)-**46**, which was reused in up to nine subsequent runs and afforded (*S*)-1-phenylpropane-1-ol without loss of chiral induction.[28c] The protonation of the Sm^{III}-enolate, obtained from 2-methoxy-2-phenylcyclohexanone, afforded the corresponding enantioenriched ketone with similar yields and ees by using both (R_a,*S*,*S*)-**47** and its non-fluorinated analogue.[30] The main advantage of (R_a,*S*,*S*)-**47** is its easy recyclability *via* a simple filtration. The enantioselective fluorescent recognition of *trans*-1,2-diaminocyclohexane was performed using a fluorous BINOL in an FC-72/MeOH biphasic system.[31]

The success encountered with the axially chiral BINOL-type ligand fostered the development of designer diol ligands, *i.e.*, (R_a,*R*,*R*)-**58**,[32] (R_a,*R*,*R*)-**59**,[32a–c] and (R_a,*R*,*R*)-**60**,[32a,b,33] bearing benzylic α-C_nF_{n+1}-alcohols, whose acidities are closely similar to the ones of phenolic compounds. The Ti^{IV}-catalyzed addition of Et_2Zn to benzaldehyde **48** was tackled to evaluate the increase of the steric bulk arising from the various perfluoroalkyl chains (Scheme 7).[32a] The highest enantiomeric excess of (*S*)-**53** was obtained using (R_a,*R*,*R*)-**60**, where the C_7F_{15} chains were inducing maximum steric hindrance. Moreover, the (R_a,*R*,*R*)-**60**/Ti^{IV} catalytic system was profitably applied in fluorous catalysis, and the chiral ligand was recovered quantitatively over seven cycles using an optimized binary solvent system of FC-72/CH_2Cl_2 (2 : 1).[33b]

Overall, the increase in acidity of hydroxylic groups is a direct effect from the incorporation of fluorine atoms onto chiral ligands. Similarly, electronically deficient *O*-binding sites allow better interactions with the metal involved giving a more compact TS, resulting in an increased asymmetric induction and even in a complete reversal of it. Perfluoroalkyl chains have provided chiral ligands the ability to be recycled through various fluorous phase extraction strategies.

2.2 *N,O*-Based binding modes

2.2.1 Diols. A sterically hindered catalytic site was built from 2,2′-bipyridinediol (*S*,*S*)-**61** to take advantage of the stereoelectronic properties of CF_3 groups at the α,α′-positions of the OH moieties. A selection of aromatic, heteroaromatic, and aliphatic alcohols (*R*)-**53**, (*R*)-**55**, and **70–77** were obtained in good to excellent yields (up to 99%) and enantioselectivities (up to 95% ee) using a Zn^{II}-mediated reaction (Scheme 8).[34] As observed from X-ray diffraction (XRD) analysis, the hexacoordinated (*R*,*R*)-**61**/$Zn(OTf)_2$ complex led to the hypothesis of coherent transition state models of distinct configurations – either as *exo–trans* or *endo–trans* – giving the major and minor enantiomers, respectively. Interestingly, (*S*)-ibuprofen was employed for the resolution of the α-CF_3-alcohols, and *2,2′-bipydiol* **61** was synthesized in both enantiomeric forms with excellent stereoselectivities (97% de and >99% ee for *R*,*R*; >99.5% de and >99.5% ee for *S*,*S*).

Chiral Schiff's base ligands (*S*)-**78–83**, containing an α-CF_3-alcohol at a *C*-stereocentre, were used in the addition of

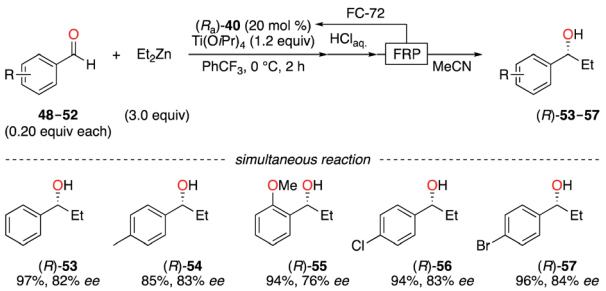

Scheme 6 Simultaneous ethylation reaction of aldehydes in FBS.

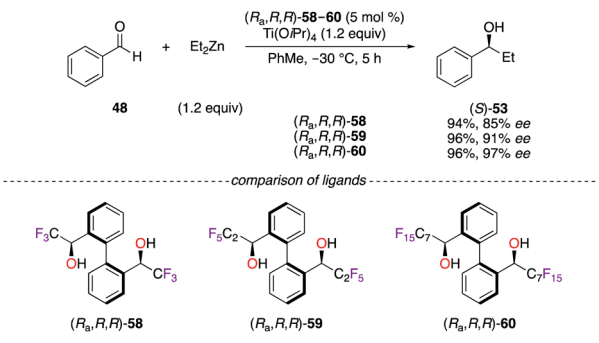

Scheme 7 Ti^{IV}-Catalyzed ethylation reaction using α,α′-C_nF_{n+1}-diol ligands.

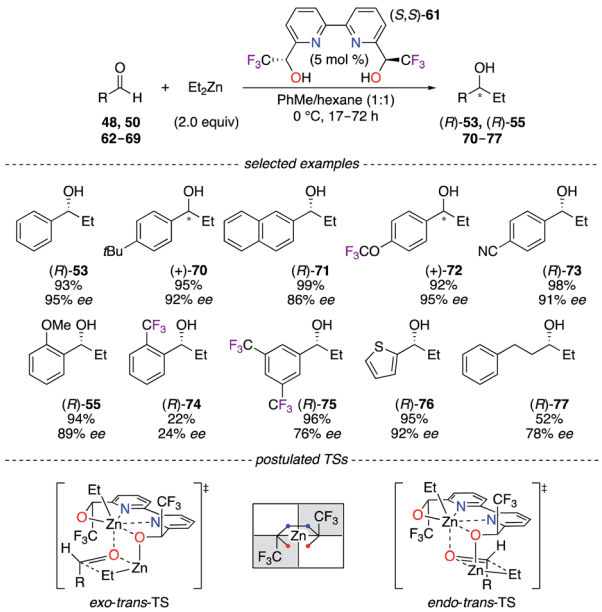

Scheme 8 2,2′-Bipyridine-α,α′-CF_3-diol/Zn^{II}-mediated ethylation reaction of aldehydes.

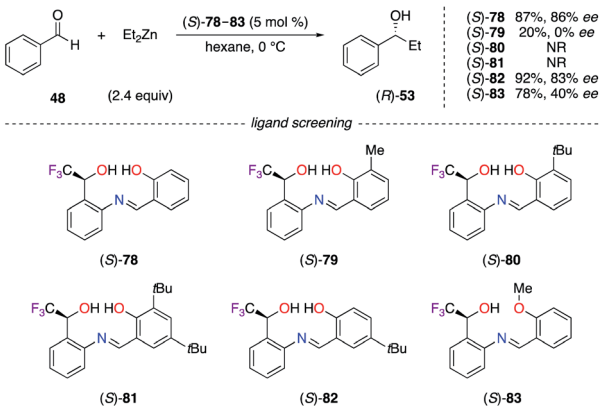

Scheme 9 Zn^{II}-Mediated ethylation reaction of **48** using Schiff's bases bearing an α-CF_3-alcohol.

diethylzinc to benzaldehyde **48** (Scheme 9).[35] Ligands (*S*)-**79–81**, substituted at the *ortho* position with a Me or a ^{t}Bu group, failed to increase the chiral induction. Only *para*-substituted (*S*)-**82** afforded (*R*)-**53** with similar ee to (*S*)-**78**. A non-linear relationship with a minimum enantiomeric amplification, together with high resolution mass spectrometry (HRMS) analysis, suggested that the dimeric $[(S)\text{-}\mathbf{78}]_2/Zn^{II}$ complex is the active catalyst. The *C*-stereocentre of Schiff's base ligands (*S*)-**78–83** was constructed by the enantioselective reduction of the *o*-nitrophenyl-α-CF_3-ketone using the (*R*)-CBS oxazaborolidine reagent. Surprisingly, the non-fluorinated analogues of these Schiff's base ligands have not been described in the literature so far.

2.2.2 β-Amino alcohols. Fluorinated β-amino alcohol ligands **84–95** have been used in various asymmetric transformations involving the alkylation of aldehydes (Scheme 10). In the Et_2Zn alkylation reaction of benzaldehyde,[36] only the organozinc catalyst prepared from (*S*)-**88** led to a maximum enantioselectivity, notwithstanding the presence of the Me or ^{i}Pr substituents on the ligand at the α-position of the hydroxyl group giving (*S*)-**89** and (*S*)-**90** with bulkier quaternary carbon stereocentres (Scheme 10, left). Correlation studies on the catalyst loading (2–50 mol%) have demonstrated a strong dependence between the increased amount of (*S*)-**88–90** and the ee observed on (*R*)-**53**, whereas no dependency was determined for the non-fluorinated analogues (*S*)-**94** and (*S*)-**95**; the superior degree of aggregation of CF_3-containing β-amino alcohol ligands, particularly for the $(S)\text{-}\mathbf{88}/Zn^{II}$ catalyst, strongly participated in the mechanism to reach higher chiral induction of alcohol (*R*)-**53**.[36a] A wider library of β-amino α-CF_3-alcohol ligands were screened in the Reformatsky reaction of PhCHO (Scheme 10, right).[37] The ees obtained with ligands (*S*)-**84** and (*S*)-**85**, containing a primary or a secondary amine, were much lower than the ones provided using tertiary amine-based ligands. Furthermore, (*S*)-**86** possessing a *N*,*N*-dimethyl-amino group led to the highest 81% ee of (*R*)-**96** in comparison with the other ligands having diisopropylamine ((*S*)-**87**), piperidine ((*S*)-**88**), and carbazole ((*S*)-**91**) motifs at the β-position. As shown on (*S*,*S*)-**92** and (*S*,*S*)-**93**, the benzene ring bearing β-amino α-CF_3-alcohols tethered at the 1,2 and 1,3 positions were considerably less efficient than (*S*)-**86**. The aggregation effect of

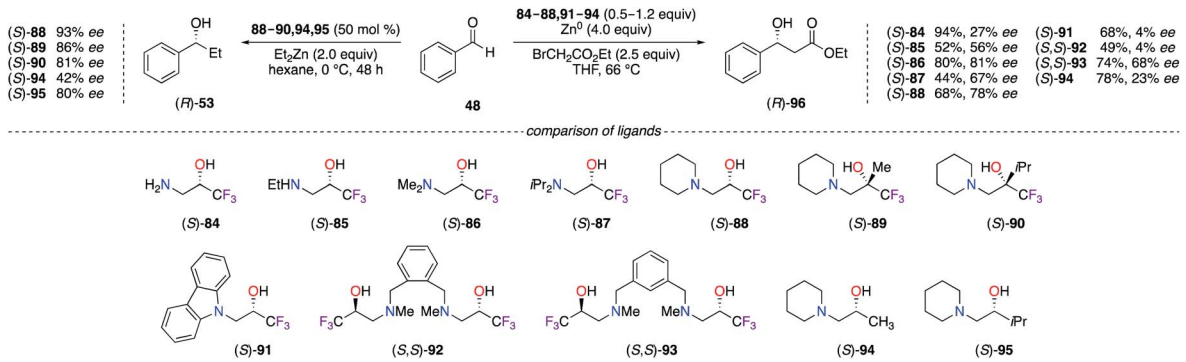

Scheme 10 Et_2Zn alkylation (left) and Reformatsky (right) reactions of benzaldehyde using amino-alcohol derivatives.

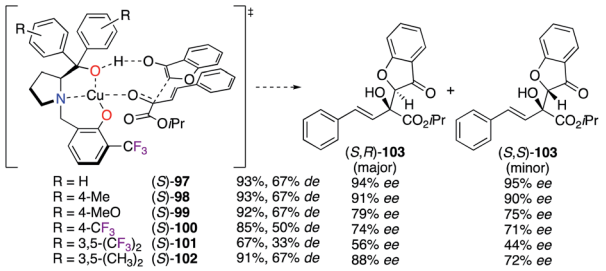

Scheme 11 Postulated TS for the Cu^{II}-catalyzed aldol reaction.

such trifluoromethylated ligands with Zn^{II} species was also found beneficial for the enantioselectivity ((*S*)-**88** *vs.* (*S*)-**94**).

Zn^{II}-Catalyzed alkylation of aldehydes was also performed using substituted *N*-methyl-L-prolinol bearing α,α-aryl groups substituted by a F atom[38] or a C_8F_{17} chain[39] at the *para* position. Through Ag^{I} catalysis, the 1,3-dipolar cycloaddition reaction was disclosed using 2,3-dihydroimidazo[1,2-*a*]pyridine-based DHIPOH ligands, substituted by a CF_3 group at the C6 position of the quinoline backbone, but they only showed modest chiral inductions among the tested ligands.[40]

The Cu^{II}-catalyzed aldol reaction of β,γ-unsaturated α-ketoesters with coumarin-3-ones was investigated using various prolinol derivatives (*S*)-**97–102**(Scheme 11).[41] Supported by density-functional theory (DFT) calculations, the nucleophilic attack of coumarin-3-one was hypothesized to occur from the *Si*-face of the α-ketoester in order to prepare predominantly the *S*,*R* diastereoisomer of **103** with good yields (67–93%) and low to excellent enantioselectivities (56–94% ee). According to the experimental results, the values of the observed ees were decreased when electron withdrawing groups were present on the aromatic rings.

The Brønsted base/Lewis acid cooperative catalysis was highlighted by the formation of dinuclear Zn^{II} catalysts in the presence of bis(prolinol)phenols (*S*,*S*)-**104–106** (Fig. 5).[42] Unfortunately, lower stereoselectivities were obtained using (*S*,*S*)-**104–106** *vs.* the non-fluorinated ligands in both the alkynylation[43] and the domino Michael/Mannich [3 + 2] cycloaddition reactions.[44]

2.2.3 β-Amido chalcogens. *N*-Polyfluoroacyl β-chalcogeno amide ligands (*S*)-**107–113** were employed conjointly with a Pd^{II} salt in the asymmetric allylic alkylation reaction of *rac*-**114** using dimethyl malonate **115** (Scheme 12).[45] Ligand (*S*)-**107** containing a sulfur atom provided (*R*)-**116** with the best enantioselectivity among the chalcogen series (S > Se > Te). Additionally,

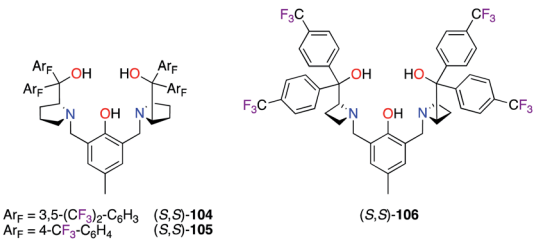

Fig. 5 Fluorinated bis(prolinol)phenol-type of ligands.

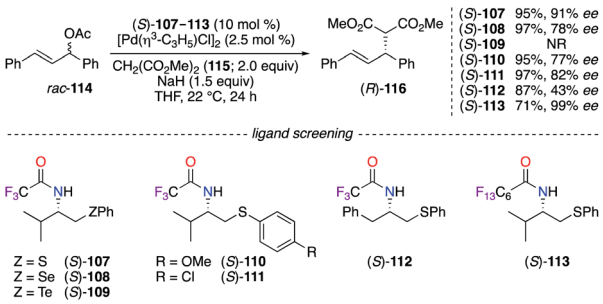

Scheme 12 β-Amido chalcogen/Pd^{II}-catalyzed asymmetric allylic alkylation reaction.

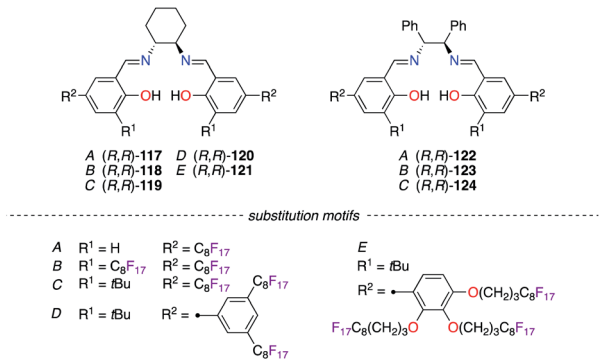

Fig. 6 Salen ligands bearing fluorinated motifs.

modifications of the electronic nature of the thioether group ((*S*)-**110**, (*S*)-**111**) and the side chain attached to the stereocentre ((*S*)-**112**) failed to improve the level of chiral induction. Surprisingly, an excellent 99% ee was observed on (*R*)-**116** when a perfluorinated amide group was introduced on the optimal skeleton of ligand (*S*)-**113**, which was recovered by a liquid–liquid extraction and was further employed in a subsequent allylic alkylation reaction with no loss of chiral induction.

2.2.4 Salens. Condensation of numerous fluorous salicylaldehydes (A–E) with (*R*,*R*)-1,2-diaminocyclohexane (DACH) and (*R*,*R*)-1,2-diphenylethylenediamine (DPEN) generated salen ligands (*R*,*R*)-**117–121** and (*R*,*R*)-**122–124** (Fig. 6). Both types of

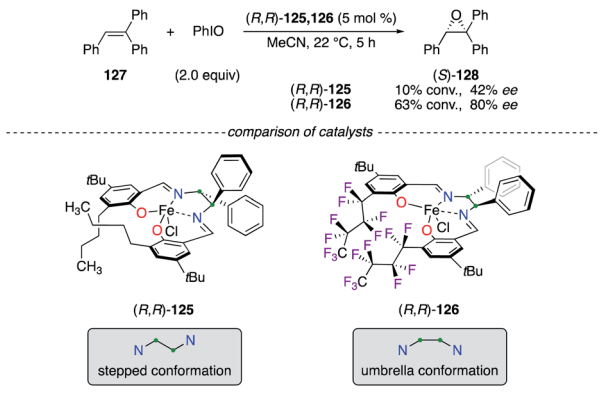

Scheme 13 PhIO-assisted epoxidation reaction using chiral Fe^{III} complexes.

ligands were mixed with Mn^{III},[46] Co^{II},[47] or Ir^{II} salts,[48] and these salen/metal catalysts showed high levels of stereoinduction in various catalytic applications using FBS.

The efficiency of Fe^{III}(salen) catalysts was compared in the asymmetric epoxidation reaction of **127**, from which a higher level of chiral induction was mainly attributed to the fluorophilic effect (Scheme 13).[49] According to crystallographic experiments, two distinct structures of the catalyst (*R*,*R*)-**125** and (*R*,*R*)-**126**, bearing respectively C_4H_9 and C_4F_9 chains, were presented. Catalyst (*R*,*R*)-**126**, because of intramolecular stacking of the C_4F_9 chains arising in it, was described to adopt a unique umbrella conformation, which was more efficient to afford enantiomerically enriched (*S*)-**128** than the usual C_2-symmetrical stepped conformation of metal(salen) complexes.

Structural insights into the C_2-symmetric complexes prepared from the combination of fluorous diamino–dialkoxy ligands and Ti^{IV} and Zr^{IV} cations were obtained from various spectroscopic and crystallographic analyses.[50]

2.2.5 Carboxamidates. Tetrakis(carboxamidates) derivatives of chiral dirhodium catalysts **129–131**, bearing α,α-fluorine atoms, were developed by Doyle to increase the catalytic activity, while maintaining high levels of asymmetric induction for selected transformations: (i) insertion reaction into the Si–H bond (left), (ii) intramolecular cyclopropanation (up), and (iii) ylide formation/[2,3]-sigmatropic rearrangement (right) reactions (Scheme 14).[51] All tested catalysts, (*S*)-**129**, (*R*)-**130**, and (*R*)-**131**, showed increased reactivity towards diazo compounds **19**, **133**, and **135**, although the stereoselectivities of products **132**, (*S*,*R*)-**134**, **136**, and **137** were lower than the ones obtained with their corresponding non-fluorinated analogues.

Chiral dirhodium catalyst *P-cis–anti*-**139** was employed in the [2 + 1]-cycloaddition reaction of ethyl α-diazoacetate **135** and hept-1-yne **140** (Scheme 15).[52] Other mono- and tris(amidate)-bridged Rh^{II}_2 complexes were prepared from the *N*-triflylimidazolidinone precursor (*R*,*R*)-**138**, but all led to (*S*)-**141** with lower enantioselectivities (<95% ee). The *trans*-vicinal CF_3 groups on the imidazolidinone backbone brought up interesting features to (*R*,*R*)-**138**, *i.e.*, high sterically hindered and electron deficient chelating N atoms.

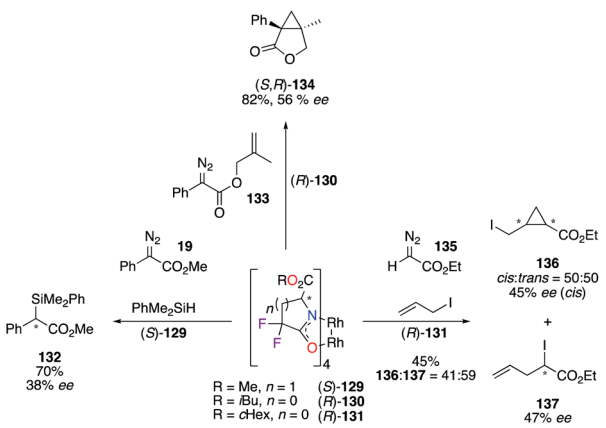

Scheme 14 Various applications of chiral Rh^{II}_2 catalysts in diazo chemistry.

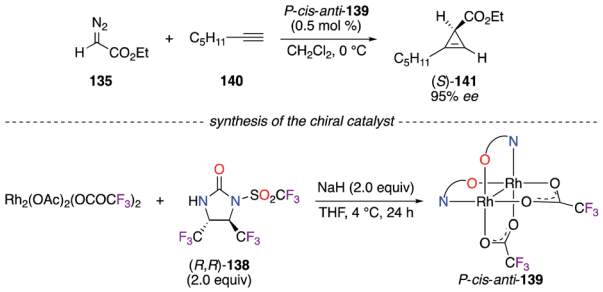

Scheme 15 [2 + 1]-Cycloaddition reaction catalyzed by the [(*R*,*R*)-**138**]$_2$/Rh^{II}_2 complex.

To sum up, ligands bearing a trifluoromethyl substituent for inducing chirality are scarce, but the potential of using the CF_3 group to provide an important steric hindrance at the α position of alcohols and amines has been disclosed in various studies. Furthermore, the beneficial synergy of both the steric and the electronic properties for optimal enantioselectivity was demonstrated in the comparison study performed using CF_3-containing ligand **88** and its Me- and ^{i}Pr-analogs in the ethylation reaction of benzaldehyde. The fluorophilic effect is also responsible for significant conformational changes to classical salen complexes leading to a new conformation adopted by the F-tagged ligand–metal complex.

2.3 *N*-Based binding modes

2.3.1 Diamines and diimines. Chiral 1,2-diaminocyclohexane (DACH)-derived diimine ligands (*R*,*R*)-**142–147** have been promoted in asymmetric catalysis in the pioneering work by Jacobsen in both the olefin aziridination and the carbene insertion into the Si–H bond (Fig. 7).[53] In Cu^{II} catalysis, Evans described the Diels–Alder reaction of 3-acryloyl-2-oxazolidinone **148** with cyclopentadiene **14** as being highly enantioselective when (*R*,*R*)-**142**, bearing two 2,6-

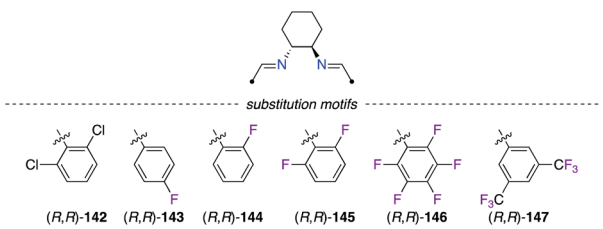

Fig. 7 Fluorinated motifs incorporated into DACH-type diimine ligands.

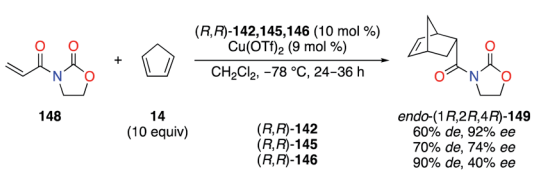

Scheme 16 Cu^{II}-Catalyzed Diels–Alder reaction – diimine ligand screening.

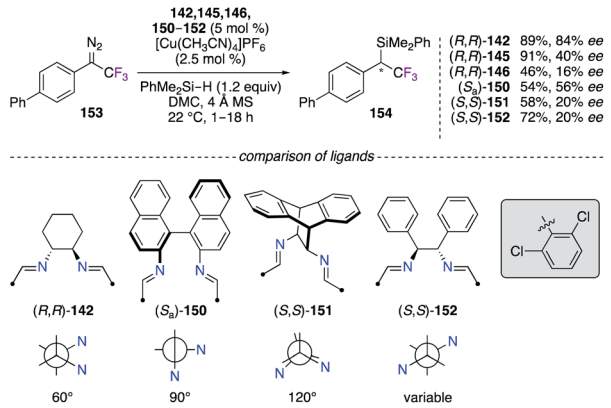

Scheme 17 Cu^{I}-Catalyzed carbene insertion reaction into the Si–H bond – chiral diimine possessing various bite angles.

dichlorophenyl arms, was used (Scheme 16).[54] Interestingly, fluorine substitution at the 2,6- and 2,3,4,5,6-positions of the aryl group led to lower enantioselectivities of (1*R*,2*R*,4*R*)-**149**, but higher *endo*/*exo* diastereoselectivities were observed (**142** < **145** < **146**).

The insertion reaction of 1-(1,1′-biphenyl)-2,2,2-trifluoro-1-diazo-ethane **153** into $PhMe_2Si$–H was performed using chiral diimine Cu^{I} complexes (Scheme 17).[55] In comparison with the best 84% ee obtained with (*R*,*R*)-**142**, the fluorinated diimine analogues (*R*,*R*)-**145** and (*R*,*R*)-**146** led to unsatisfactory 40% ee and 16% ee, respectively. Being very interested towards a ligand design approach, 2,6-dichlorobenzaldehyde and other chiral diamine scaffolds, *i.e.*, (S_a)-1,1′-binaphthyl-2,2′-diamine, (*S*,*S*)-11,12-diamino-9,10-dihydro-9,10-ethanoanthracene, and (*S*,*S*)-DPEN, were condensed together to generate new diimine-type ligands with distinct bite angles.[56] However, the **150–152**/Cu^{I} catalysts failed to give the insertion product with higher enantioselectivities than (*R*,*R*)-**142**. As shown in this study, any mix-and-match combinations involving a chiral diamine precursor and a desired aldehyde could lead to potential candidates being used for chiral induction.

Chiral diamine ligands are prepared from the simple reductive amination of diimine precursors, *e.g.*, using sodium borohydride.[57] Numerous aldehydes containing different *F*-patterns were first treated with (*R*,*R*)-DACH and then reduced

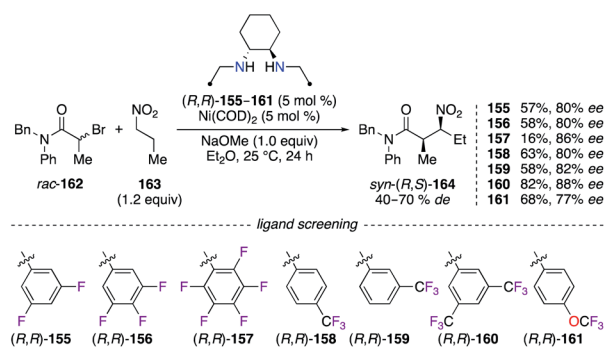

Scheme 18 Ni^{0}-Catalyzed *C*-alkylation reaction – optimization of the chiral diamine ligand.

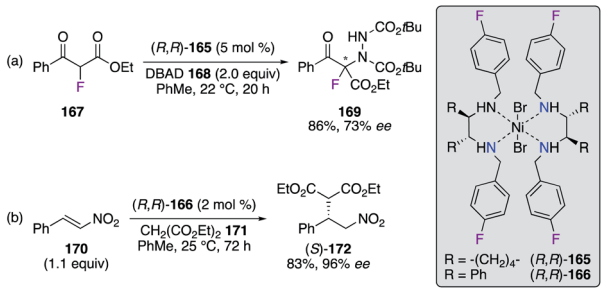

Scheme 19 Ni^{II} complexes employed in addition-type reactions.

with $NaBH_4$ or $NaBH(OAc)_3$, to give chiral 1,2-diamine ligands (*R*,*R*)-**155–161**. The ability for chiral induction of these electronically deficient ligands was studied in the Ni^{0}-catalyzed *C*-alkylation reaction of 1-nitropropane **163** by α-bromoamide *rac*-**162** (Scheme 18).[58] Independent of the nature of the substituent (F, CF_3, or OCF_3), fluorine substitution at the 3-, 4-, 2,6-, and 3,4,5-positions of the aromatic ring afforded *syn*-(*R*,*S*)-**164** with up to 82% ee, whereas a good 86% ee, together with a low 16% yield, was observed when using the C_6F_5 analogue. Optimal results were obtained with the (*R*,*R*)-**160**/Ni^{0} system, and this catalyst was proven highly efficient to prepare 26 β-nitroamides with excellent stereoselectivities (up to 90% de_{syn} and 99% ee_{syn}).

Chiral DACH- and DPEN-based Ni^{II} complexes (*R*,*R*)-**165** and (*R*,*R*)-**166** with *N*,*N*′-4-fluorobenzylamine arms were employed as moisture- and air-stable pre-catalysts in enantioselective transformations (Scheme 19). The α-hydrazination reaction of α-fluoro-β-ketoester **167** with di-*tert*-butyl azodicarboxylate (DBAD) **168** was successfully performed using (*R*,*R*)-**165**, where α-amino-β-ketoester **169** was obtained in 86% yield and 73% ee (Scheme 19, eqn (a)).[59] Similarly, the (*R*,*R*)-**166**-catalyzed conjugate addition reaction of diethyl malonate **171** to β-nitrostyrene **170** was reported to give an excellent enantioselectivity on Michael adduct (*S*)-**172** (Scheme 19, eqn (b)).[60] When using 1-nitropent-1-ene as the substrate, (*R*,*R*)-**166** afforded promising 89% ee of (*R*)-diethyl 2-(1-nitropenthan-2-yl)malonate, which is a key

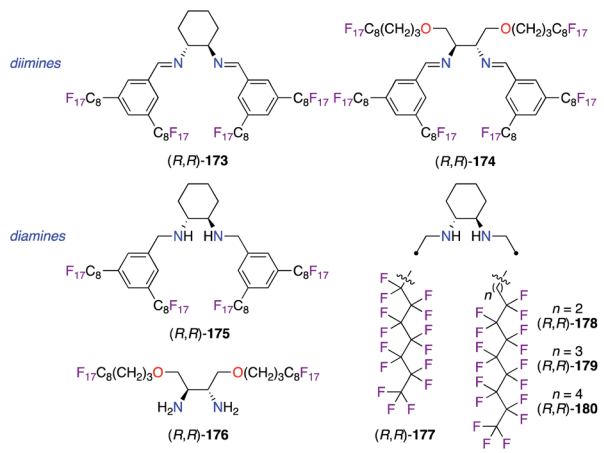

Fig. 8 Perfluorinated motifs in chiral diamine- and diimine-based ligands.

intermediate in the synthesis of brivaracetam having antiepileptic properties.

Polyfluorinated diamine and diimine types of ligands were obtained by the incorporation of perfluoalkyl chains to be used in various synthetic applications involving fluorous biphasic systems (Fig. 8). Chiral perfluorinated DACH-type diamine ligand (*R*,*R*)-**175** was more tolerant towards decomposition *vs.* diimine (*R*,*R*)-**173** over the recycling of both Ir^{I} and Cu^{I} catalysts.[48,61] In terms of chiral induction, the (*R*,*R*)-**175**/Cu^{I} catalyst afforded the *trans*-(1*R*,2*R*)-cyclopropane, obtained from styrene **20** and ethyl α-diazoacetate **135**, in 62% ee, whereas a low 6% ee of the opposite 1*S*,2*S* enantiomer was observed when using the diimine analogue. Furthermore, non-cyclic C_2-symmetric tertiary diamines also led to poor levels of enantioselectivity (*ca.* 15% ee) probably due to a too flexible environment around the Cu^{I} centre. Starting from (4*R*,5*R*)-2,2-dimethyl-1,3-dioxolane-4,5-dimethanol, the incorporation of C_8F_{17} ponytails tethered to the stereogenic carbons of the 1,2-diamine core allowed the preparation of unique fluorous diimine and diamine ligands. Unfortunately, poor levels of stereoinduction were obtained in the ATH reaction of acetophenone in a fluorous solvent using either Ir^{I} or Ru^{II} catalysts made from (*R*,*R*)-**174** or (*R*,*R*)-**176**.[62] Alternatively, the introduction of perfluoro-heptyl and -octyl chains directly on both N atoms led to aliphatic diaminocyclohexane (*R*,*R*)-**177–180**, which were found promising only in the Cu^{I}-catalyzed cyclopropanation of styrene **20** among the tested reactions.[63]

Overall, the 1,2-diphenylethylenediamine scaffold is scarcely described in the literature for the synthesis of fluorinated diimine and diamine ligands. To overcome this situation, an efficient method was described for the synthesis of DPEN-type ligands with diaryl-substituted backbones *via* a diaza-Cope rearrangement of (*S*,*S*)-1,2-bis-(2-hydroxyphenyl)-ethylenediamine **181** (or (*R*,*R*)-**181**) in the presence of the desired aldehyde.[64] Following the described protocol, fluorinated DPEN (*R*,*R*)-**185–187** were synthesized in high yields (77–87%) *via* the condensation of (*S*,*S*)-**181** with aldehyde **182–184**, *i.e.*, 4-F-C_6H_4-CHO, C_6F_5-CHO, and 4-CF_3-C_6H_4-CHO (Scheme 20). The diaza-Cope rearrangement was postulated to proceed through a six-membered chair transition state giving the desired diimines with chiral inversion of the *C*-stereocentres. This method is highly useful for the preparation of

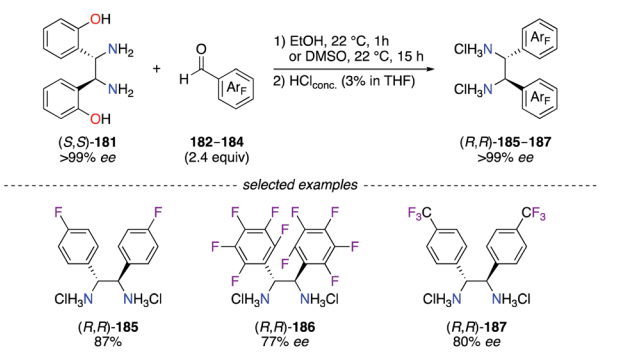

Scheme 20 Stereospecific preparation of C_2-symmetric fluorinated DPEN ligands.

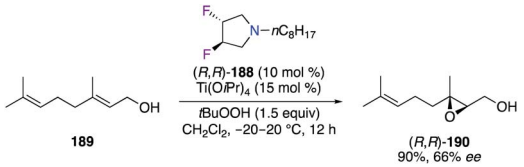

Scheme 21 Ti^{IV}-Catalyzed epoxidation reaction of geraniol.

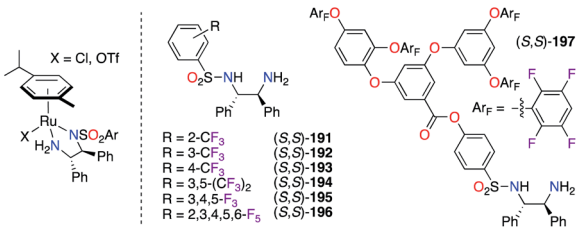

Fig. 9 F-containing tosylated-(*S*,*S*)-DPEN ligands in Ru^{II} complexes.

F-containing DPENs, which could be used as enantiopure building blocks – either as the *R*,*R*, or the *S*,*S* – to give diimine- and diamine-based designer ligands.

Trans-(*R*,*R*)-3,4-difluoropyrrolidine (*R*,*R*)-**188**, used as monodentate amine, was combined with $Ti(O^{i}Pr)_4$ to catalyze the epoxidation of geraniol **189**, giving the corresponding epoxide (*R*,*R*)-**190** with a moderate 66% ee (Scheme 21).[65]

2.3.2 Sulfonamides. The sulfonylation of simple DPEN ligands with various aromatic sulfonyl precursors where fluorine substitution appears on all carbons of the aryl paved the way to a wide library of *N*-(tosyl)-1,2-phenylethylenediamine (TsDPEN) ligands (*S*,*S*)-**191–197** (Fig. 9). Their complexation with Ru^{II} salts was proven valuable for both the tandem hydration/asymmetric transfer hydrogenation (ATH) of alkynes[66] and the asymmetric hydrogenation (AH) of bisquinoline,[67] where (*S*,*S*)-**191–196** and (*R*,*R*)-**193** were respectively used. Fluorous dendritic (*S*,*S*)-**197** showed an enhanced activity and recyclability of the Ru^{II} catalyst towards the ATH reaction of aromatic ketones into secondary alcohols, which were obtained with excellent ees.[68] During the optimization of the reaction conditions, (*R*,*R*)-**193** and (*R*,*R*)-**194** were screened, but the latter

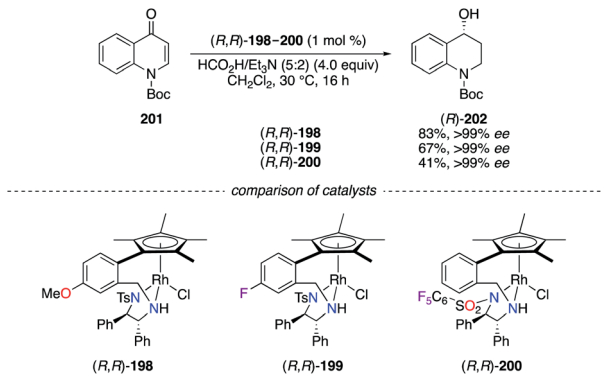

Scheme 22 Rh^{III}-Catalyzed ATH reaction of **201** into (*R*)-**202**.

was chosen as the optimal chiral ligand in the Ir^{III}-catalyzed ATH reaction of 2,9-dimethyl-1,10-phenanthroline.[69]

The ATH of *N*-protected 4-quinolone **201** using the formic acid/triethylamine mixture as the hydrogen source was performed using chiral Rh^{III} complexes (*R*,*R*)-**198–200** (Scheme 22).[70] All three catalysts afforded excellent chiral inductions, but the partial cleavage of the *tert*-butyloxycarbonyl (Boc) group occurred when using a stronger Lewis acidic catalyst; hence lower yields of (*R*)-**202** were obtained using (*R*,*R*)-**199** and (*R*,*R*)-**200**.

A 3,5-ditrifluoromethylated phenyl ring was incorporated into a Cinchona-alkaloid-based sulfonamide ligand, which was employed as the chiral source in the Cu^{II}-catalyzed radical oxytrifluoromethylation of alkenyl oximes.[71] The Simmons-Smith cyclopropanation of allylic alcohols was performed using *in situ* generated Zn^{II} complexes from fluorous disulfonamide ligands, where both ligands were easily recovered by fluorous solid phase extraction.[72]

2.3.3 Imidazolines. The (*S*,*S*)-DPEN scaffold was further employed as the chiral synthon for the synthesis of imidazoline-based ligands in the highly enantioselective Friedel–Crafts alkylation reaction of indoles with ethyl 3,3,3-trifluoropyruvate **208** (Scheme 23).[73] Among them, fluorous phenylene bis(imidazoline) (PheBIM) bis-(*S*,*S*)-**203–206** – particularly ligands bis-(*S*,*S*)-**203** and bis-(*S*,*S*)-**206** possessing a CF_3 group at the *para* position of the phenyl ring – afforded **209** with good enantioselectivities when indole **207** was used as the nucleophile.

The allenylation of terminal alkynes and diazo compounds, generated *in situ* by MnO_2-assisted oxidation of their corresponding hydrazone in a continuous flow system, was disclosed as being highly enantioselective (89–97% ee) under Cu^{I} catalysis (Scheme 24).[74] A library of pyridine bis(imidazoline) (PyBIM) ligands bearing *N*-aryl substituents, *i.e.*, 4-CF_3-C_6H_4, 3,5-$(CF_3)_2$-C_6H_3, and 4-CF_3-3,5-F_2-C_6H_2, was screened, but only (*S*,*S*)-**210**, comprising 4-SF_5-C_6H_4 groups, showed an optimal chiral induction. Noteworthily, these chiral ligands were synthesized

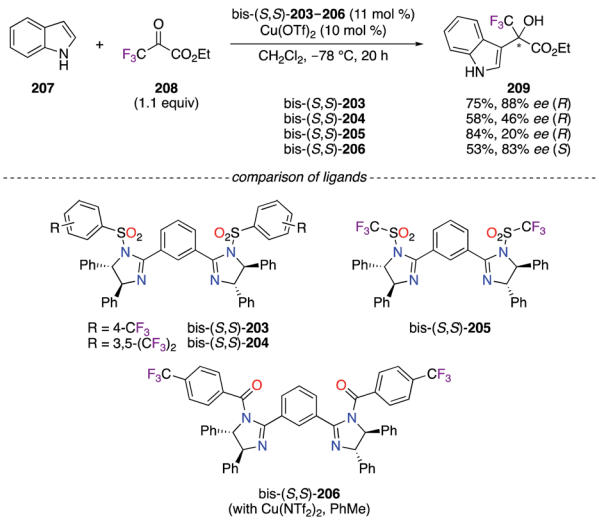

Scheme 23 Friedel–Crafts alkylation reaction using chiral PHEBIM ligands.

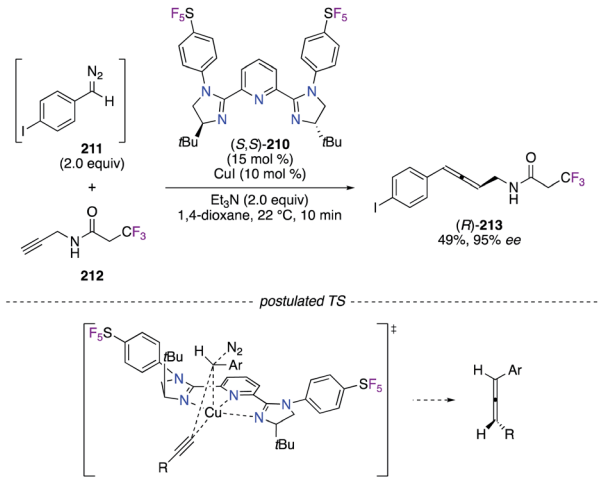

Scheme 24 Cu^{I}-Catalyzed allenylation reaction and the postulated TS.

from the treatment of a pyridine-2,6-diimidoyl chloride precursor, derived from (*S*)-*tert*-leucinol, with the corresponding fluorinated aniline, such as 4-(pentafluorothio)aniline in the case of (*S*,*S*)-**210**. As postulated, enantioenriched allene (*R*)-**213** was synthesized *via* the concerted Cu–C bond insertion of the (*S*,*S*)-**210**/Cu^{I} acetylide intermediate into the diazo compound **211**, which approaches with the H near the ^{t}Bu group of the ligand to induce minimal steric strains. The scope was further extended to propargylamides derived from (*S*)-ibuprofen, penicillin G, (*R*,*R*)-atorvastatin, and others, and excellent stereoselectivities were highlighted in the disclosed method.

2.3.4 Oxazolines. Tetrahydrofuran derivatives were synthesized with excellent stereoselectivities *via* the [3 + 2] cycloaddition of racemic cyclopropanes with various aldehydes using a ^{t}Bu–pyridine bis(oxazoline) (PyBOX) ligand.[75] The selection of electronically modified *para*-substituted ^{t}Bu-PyBOX ligands (*S*,*S*)-**214–216** has induced significant alteration of the yields rather than the ees, even though (*S*,*S*)-**215** afforded 2,5-diaryl-THF (*R*,*R*)-**218** with the best enantiocontrol (Scheme 25). However, the *p*-Cl-^{t}Bu-PyBOX showed a slightly better efficiency (74% yield, >98% de, 92% ee) and, therefore, was chosen to

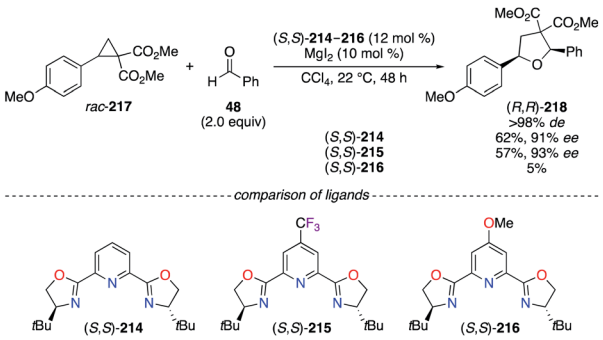

Scheme 25 Mg^{II}-Catalyzed dynamic kinetic asymmetric [3 + 2] cycloaddition reaction.

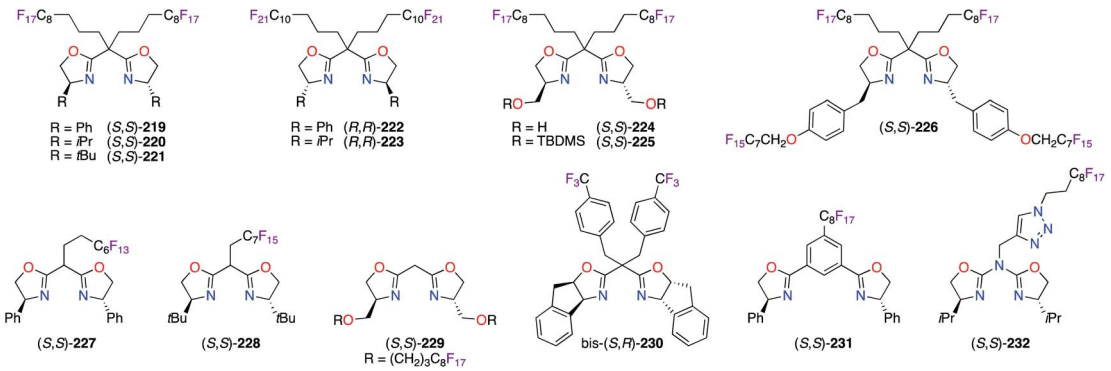

Fig. 10 Fluorous chiral bis(oxazoline)-derived ligands.

evaluate the scope of the reaction. An opposite trend was observed in the Cu^{I}-catalyzed allenylation reaction presented above, where the optimization studies performed on model substrates, using *p*-R-^{i}Pr-PyBOX ligands instead of ^{t}Bu-PyBOX, led to the corresponding allene with 47% ee (R = CF_3), 68% ee (R = H), and 70% ee (R = OMe).[74]

Chiral pyridine(oxazoline) (PyOX) ligands bearing a CF_3-substituted C5 position were tested, but virtually no conversion was noted in the Pd^{II}-catalyzed dihydroxylation reaction of catechol and *trans*-1-phenyl-1,3-butadiene.[76] Other examples of mono-oxazoline tethered CF_3-based ligands were presented as amido-oxazolinate/Zn^{II} and sulfoxide-oxazoline/Pd^{II} complexes.[77]

Similarly, fluorous bis(oxazoline) (BOX) ligands were synthesized and used with various metals to attain solubilization of the obtained chiral catalysts in fluorous solvents (Fig. 10). Starting from simple BOX derivatives, the incorporation of perfluoroalkyl substituents, comprising C_8F_{17} and $C_{10}F_{21}$ chains, on the methylene bridge afforded (*S*,*S*)-**219–221** and (*R*,*R*)-**222** and (*R*,*R*)-**223**. High ees were obtained using these chiral ligands in the Pd^{II}-catalyzed allylic alkylation,[78] Cu^{I}-catalyzed allylic oxidation[78b] and cyclopropanation,[79] and Cu^{II}-catalyzed ene[80] reactions. Used in these reactions, (*S*,*S*)-**224** and (*S*,*S*)-**225** both showed a favoured complexation with $[Pd(\eta^3\text{-}C_3H_5)Cl]_2$ to reach high chiral inductions, whereas low reactivity was obtained with $Cu(OTf)\cdot 0.5C_6H_6$.[78b] To facilitate the recycling of fluorinated BOX ligands, up to four perfluorooctyl chains were introduced on (*S*,*S*)-**226**, which was synthesized from (*S*)-tyrosine, to increase its fluorine content up to 59.3%.[81] Mono-perfluoroalkyl bridged BOX ligands (*S*,*S*)-**227** [82] and (*S*,*S*)-**228** [78b] were essentially designed to be used in common organic solvents for optimum catalytic activity, but to be recovered *via* a fluorous solid-phase extraction. Moving the perfluoroalkyl chains closer to the centre of chirality had no tremendous influence on the obtained ees using catalysts prepared from (*S*,*S*)-**229** together with Pd^{II} or Cu^{I} salts.[81] As part of the ligand screening, the indane-based bis-(*S*,*R*)-**230**/Cu^{II} catalyst afforded *tert*-butyl α-fluoroester with a modest 61% ee *via* the fluorination of diazoester **19**.[83] The synthetic utility of (*S*,*S*)-**231** was demonstrated in the synthesis of enantioenriched compounds bearing 3-hydroxy-2-oxindole and quinazolinone scaffolds using Cu^{II} or Sc^{III} catalysis.[82c,d] Importantly, the great ability of the triazole ring for coordination with copper salts was offset by the pefluoroalkyl group effect on azabis(oxazoline) ligand (*S*,*S*)-**232** or its $F_{51}N_9$-tripodal analogue. As a result, high enantioenrichments were afforded in the benzoylation, Friedel–Crafts alkylation, and Henry reactions.[84]

The strategy of preventing the immobilization of BOX chiral ligands onto poly(ethyleneglycol) (PEG) materials was further explored using (*S*,*S*)-**233–236** (Fig. 11). Two substitution motifs comprising perfluoroalkyl chains, A[85] or B,[86] were included in the structure of the BOX ligands. The fluorinated moieties, which were separated from the coordination sites by an appropriate spacer to reduce any undesired interactions, allowed excellent recovery and recycling of the ligands *via* practical procedures.

All things considered, the availability of many fluorinated aldehydes gives the access to a larger diversity of C_2-symmetric chiral diamine and diimine ligands. The variety of functionalization patterns brought by introducing fluorine at every carbon of the aromatic ring has facilitated the fine-tuning of the Lewis acidity of a catalyst through electronically modified properties. Chiral ligands bearing the SF_5 group have been limited due to the scarcity of the availability of the building blocks, and therefore, the pyridine bis(imidazoline) ligand is considered as a major breakthrough. Importantly, not only the recycling of chiral fluorous catalyts remains a key objective using various strategies, but the incorporation of diverse fluorous chains also led to ligand design in fluorous biphasic systems.

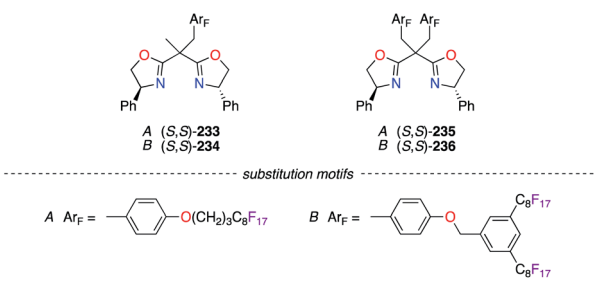

Fig. 11 Perfluoroalkyl motifs for chiral BOX ligands.

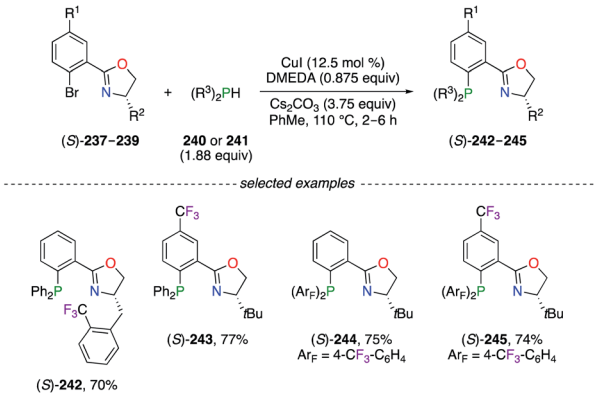

Scheme 26 Ullman-like coupling reaction for the synthesis of PHOX ligands.

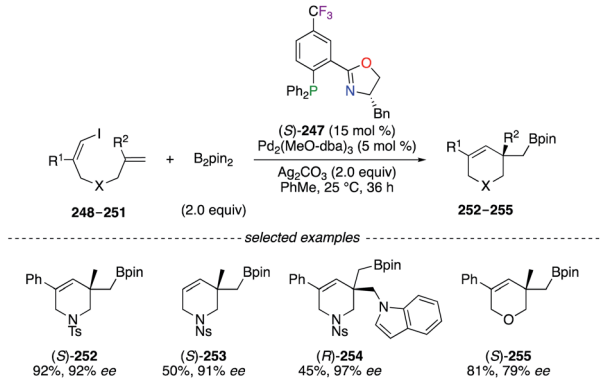

Scheme 28 (*S*)-247/Pd^0-Catalyzed vinylborylation of alkenes.

2.4 *N,P*-Based binding modes

2.4.1 Monophosphines. A wide variety of F-containing phosphino(oxazoline) (PHOX) chiral ligands were synthesized *via* the Ullmann-like coupling reaction of 2-bromo aryl derivatives (*S*)-**237–239** with the corresponding diarylphosphine (Scheme 26).[87] The simple reaction conditions, involving copper iodide and 1,2-dimethylethylenediamine (DMEDA), afforded (*S*)-**242–245** with good yields, notwithstanding the steric and the electronic properties of the substrate. Noteworthily, a considerably increased catalytic activity of the Pd^{II} catalysts was observed using (*S*)-**243** and (*S*)-**245**, which was not observed with the CF_3-substitution pattern only on the phenyl rings of (*S*)-**244**. The great utility of (*S*)-**245** was highlighted in the Pd^{II}-catalyzed intramolecular decarboxylative allylic alkylation reaction, where highly enantioenriched cyclohexanone derivatives bearing all-carbon quaternary stereocentres at the α-position were obtained with excellent yields.[87,88] Furthermore, the (*S*)-**245**/Pd^{II}-catalyzed asymmetric alkylation reaction was described as an important key step in the synthetic route of (+)-elatol, a spirobicyclic natural product belonging to the family of chamigrene.[88c] Favourable complexation with palladium salts was achieved using strong π-acceptor bis(perfluoroalkyl)phosphinooxazoline (FOX) ligands for the alkylation of monosubstituted allyl esters.[89]

The synthesis of naturally occurring and non-natural isoflavones, members of the flavonoid class, was also targeted using (*S*)-**245** through a Pd^0-catalyzed decarboxylative protonation reaction.[90] According to the postulated TS, both ^{t}Bu and MeO groups pointing upwards – from the ligand and the substrate, respectively – induce a high sterically hindered environment and lead the protonation to occur preferentially *via* the *Si*-face (Scheme 27).[90a] As a result, isoflavone (*R*)-**246** was obtained with excellent yield and enantioselectivity.

A highly enantioselective Pd^0-catalyzed vinylborylation of (*Z*)-1-iodine-dienes **248–251** with B_2pin_2 was disclosed using (*S*)-**247** for the construction of quaternary *C*-stereocentres on **252–255** (Scheme 28).[91] Interestingly, ligand screenings of non-halogenated analogues of (*S*)-**247** led to only moderate enantioselectivities (52–80% ee). Fluorinated PHOX ligands were employed in structure–reactivity correlation studies using chiral (π-allyl)palladium complexes and suggested that the electronic tuning of the ligand for maximizing both reactivity and selectivity mainly depends on the nature of the substituent rather than its position on the ligand.[92]

In the presence of $CuClO_4$, a chiral sulfinamide monophosphine (MingPhos) ligand, bearing a pentafluorophenyl substituent at the *C*-stereocentre, led to the [3 + 2]-cycloaddition product with lower enantioselectivity than its non-fluorinated analogue (66% ee *vs.* 82% ee).[93]

The Pd^{II}-catalyzed allylic alkylation reaction was performed using (*S*)-prolinol-based fluorous aminophosphine (*S*)-**256** and (*S*)-**257** (Scheme 29).[94] High enantioselectivities were obtained from the addition of dimethyl malonate **115**, at first deprotonated by LiOAc–*N*,*O*-bis(trimethylsilyl)acetamide (BSA), to 1,3-diphenyl-2-propenyl acetate *rac*-**114** by using both chiral

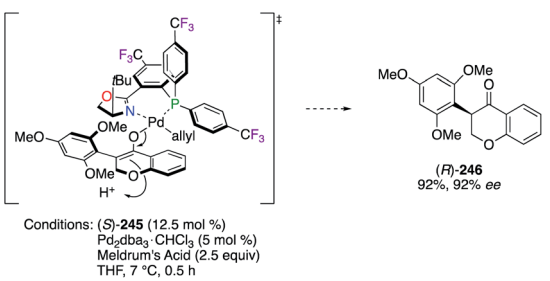

Scheme 27 Postulated TS for the synthesis of isoflavone (*R*)-**246**.

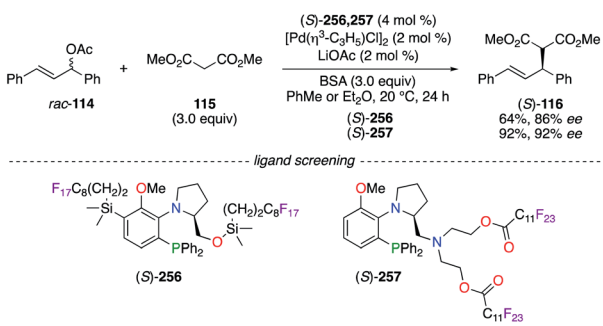

Scheme 29 Pd^{II}-Catalyzed allylic alkylation reaction using (*S*)-**256** and (*S*)-**257**.

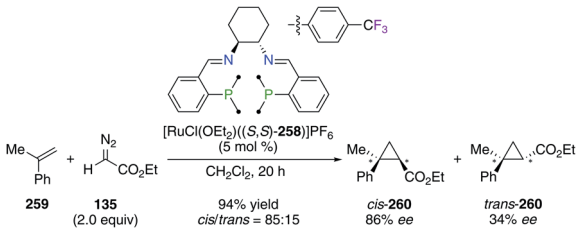

Scheme 30 Asymmetric cyclopropanation reaction catalyzed by a CF_3-containing PNNP/Ru^{II} complex.

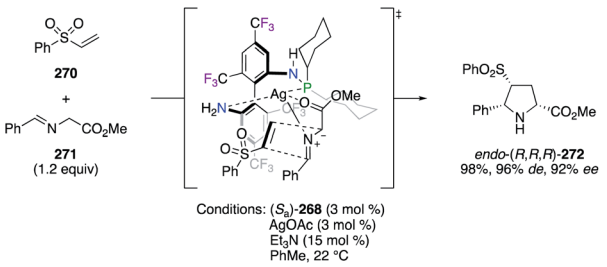

Scheme 31 Postulated TS for the attack of the azomethine ylide intermediate.

catalysts ((*S*)-**116:** 86% ee using (*S*)-**256;** 92% ee using (*S*)-**257**). The temperature-dependent solubility of the (*S*)-**257**/Pd^{II} catalyst was investigated, and these studies revealed the possibility to recover the fluorous catalyst *via* its precipitation in cold hexane.

2.4.2 Diphosphines. Fluorinated (*S*,*S*)-DACH-derived P_2N_2-tetradentate ligand (*S*,*S*)-**258** was employed in the Ru^{II}-catalyzed cyclopropanation reaction of α-methyl styrene **259** with ethyl α-diazoacetate **135** (Scheme 30).[95] The presence of 4-CF_3-C_6H_4 groups was beneficial for the synthesis of cyclopropane **260** with good 70% de_{cis}, 86% ee_{cis}, and 34% ee_{trans}, whereas the non-fluorinated analogue afforded **260** with low 52% de_{cis}, 23% ee_{cis}, and 18% ee_{trans}. When using styrene **20** and 1-octene as substrates, the [$RuCl(OEt_2)$((*S*,*S*)-**258**)]PF_6 catalyst was also highly diastereoselective for the corresponding *cis* cyclopropanes. Again, CF_3-substituted aryl groups were incorporated into a (*S*,*S*)-DPEN-based PNNP ligand, of which chiral Fe^{II} complexes were found to be highly electronically deficient, but inactive in the asymmetric transfer hydrogenation of acetophenone.[96]

2.4.3 Axially chiral monophosphines. The important *F*-containing atropisomeric 1,1′-biphenyl architecture, *i.e.*, 4,4′,6,6′-tetrakis-trifluoromethyl-biphenyl-2,2′-diamine (TF-BIPHAM) (S_a)/(R_a)-**261**, was obtained as an enantiopure material *via* the resolution of (S_a,*S*)- and (R_a,*S*)-10-camphornyl-based disulfonamide diastereoisomers and was employed in the synthesis of chiral amine–phosphine ligands (Fig. 12). The first generation of C_2-symmetric *N*,*N*′-PR_2-TF-BIPHAM ligands (S_a)-**262–265**, comprising diaryl- and dialkylphosphinyl groups, exhibited excellent asymmetric induction in the Rh^{I}-catalyzed hydrogenation of enamides.[97] Catalytic applications towards the synthesis of enantioenriched saturated heterocycles *via* a highly efficient 1,3-dipolar cycloaddition reaction, using Cu^{I} (ref. 98) or Ag^{I} (ref. 99) catalysis, were developed using the second generation of ligands. Indeed, the scope of these ligands was extended to include mono-*N*-phospanyl (TF-BIPHAMPhos) derivatives (S_a)-**266–269**. When using the (S_a)-**268**/Ag^{I} catalytic system, pyrrolidine *endo*-(*R*,*R*,*R*)-**272** was afforded in excellent yields and stereoselectivities *via* the 1,3-dipolar cycloaddition of *in situ* generated azomethine ylides, as shown using imine **271**, to vinyl sulfone **270** through the more accessible *Si* face of the imine (Scheme 31).[99b]

The Cu^{I}-catalyzed three-component alkynylation reaction from **276**, **277**, and *rac*-**278**, followed by the Au^{I}-catalyzed dehydrative cyclization reaction of alkynediol **279** into **280**, was

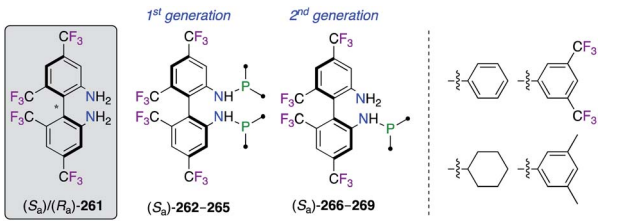

Fig. 12 Library of amine–phosphine ligands comprising the TF-BIPHAM scaffold.

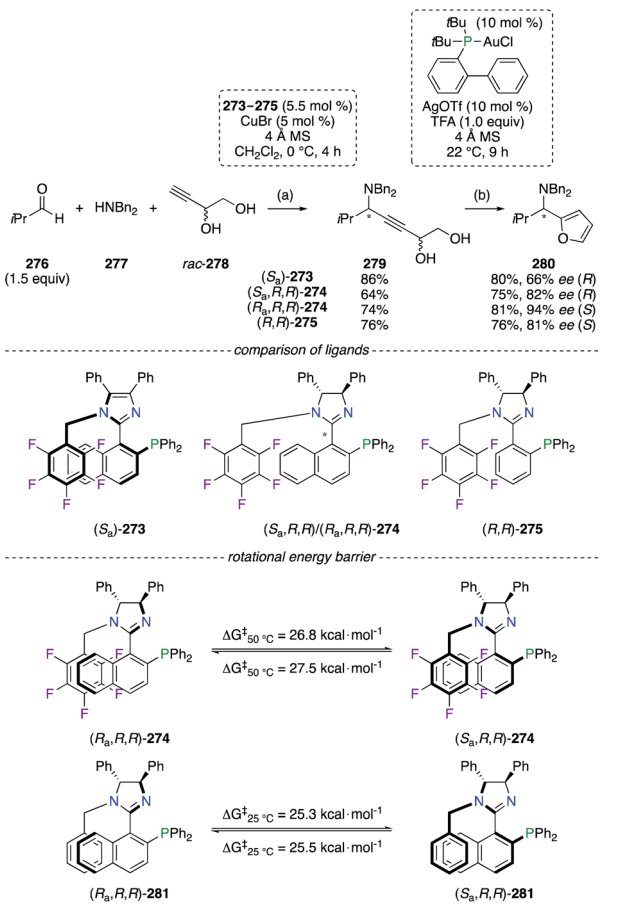

Scheme 32 Two-step synthesis of 2-aminoalkyl furan *via* the alkynylation/cyclization reaction sequence.

described as highly enantioselective using phosphino(imidazoline) (StackPHIM) (R_a,*R*,*R*)-**274** (Scheme 32).[100] Since the imidazole analogue (S_a)-**273** (StackPhos ligands)[101] and (*R*,*R*)-**275** (having no axial chirality) both led to 2-aminoalkyl furan **280** (*R* or *S*) with lower enantiomeric enrichments, the complementary between the stereocentres and the chiral axis to reach higher ee was demonstrated. Further fine-tuning of the **274**/Cu^I catalyst was highlighted by the combination of the (*R*,*R*)-DPEN scaffold with the R_a or the S_a atropisomer, resulting in an increased chiral induction of **280** from 82% ee (*R*) to 94% ee (*S*). Noteworthily, atropisomerism of configurationally stable *P*,*N*-ligands **273** and **274** arises from π,π-stacking interactions between the naphthyl and C_6F_5 moieties. Being determined experimentally at 50 °C, rotational energy barriers ($\Delta G^{\ddagger}$) of 26.8 kcal mol^{-1} (R_a into S_a) and 27.5 kcal mol^{-1} (S_a into R_a) have proven that both atropisomers of **274** could be synthesized, separated and successfully employed as chiral ligands in metal catalysis. However, the absence of fluorine atoms considerably lowered the $\Delta G^{\ddagger}$ values of R_a–S_a (or S_a–R_a) interconversion, and epimerization of **281** occurred easily even at room temperature.

2.4.4 Ferrocenes. The popular 3,5-bis(trifluoromethyl) phenyl scaffold was incorporated into chiral ferrocenyl-derived *P*,*N*-containing ligands (Fig. 13). Indeed, imine-, amine-, and oxazoline-based phosphine ligands **282–284** were successfully used in the Pd^{II}-catalyzed allylic alkylation,[102] the Rh^{II}-catalyzed hydrogenation,[103] and the Cu^I-catalyzed 1,3-dipolar cycloaddition reactions.[104] In the last case, the divergent *exo*/*endo* selectivities observed from the experimental results were rationalized through computational studies. Interestingly, the postulated TS models suggested that two different chelation modes of the substrate were arising from the electron-deficient Ar_F substituents of (S_p,*S*)-**284** *vs.* the electron-rich phenyl rings of its non-fluorinated analogue. Moreover, closely related ferrocenyl-based bis(perfluoroalkyl)phosphino(oxazoline) ligands were designed in a series of bulky ^{t}Bu, Ph and Bn substituents at the *C*-stereocentre.[89,105]

In brief, the widespread use of 4-CF_3 and 3,5-$(CF_3)_2$ motifs on the aromatic scaffold of the ligands was highlighted in this section. Importantly, the C_6F_5 group has been demonstrated as highly efficient when used in axially chiral phosphines, whereas its electrostatic pairing with the π system of the naphthyl moiety has induced a rotational energy barrier allowing atropisomerism. Also, the use of *o*,*o*′-CF_3 within the TF-BIPHAM architecture was proved valuable in this strategy.

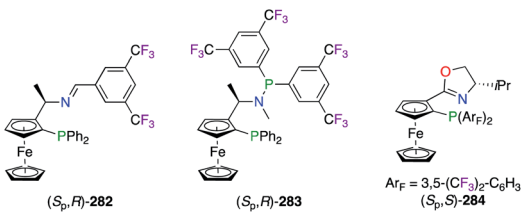

Fig. 13 Chiral ferrocenyl-derived ligands containing the 3,5-$(CF_3)_2$-C_6H_3 group.

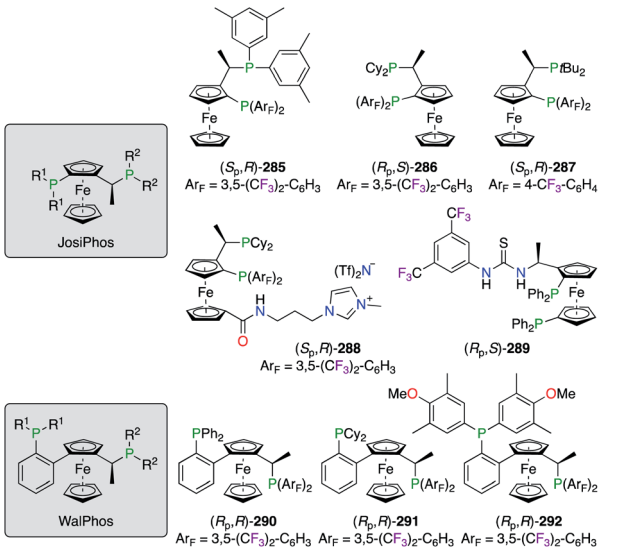

Fig. 14 Fluorinated JosiPhos- and WalPhos-type of ligands.

2.5 *P*-Based binding modes

2.5.1 Planar chiral diphosphines. Electron-poor diphosphine ligands were described for JosiPhos- and WalPhos-type ferrocenes **285–289** and (R_p,*R*)-**290–292**, respectively (Fig. 14). Chiral ligands (S_p,*R*)-**285**,[106] (R_p,*S*)-**286**,[106a,107] and (S_p,*R*)-**287** [106b] were tested in the Ir^I- or Rh^{III}-catalyzed hydrogenation and the Pd^{II}/Cu^I-co-catalyzed Heck/Sonogashira asymmetric reactions, but only high chiral inductions were obtained by using the (R_p,*S*)-**286**/Pd^{II} catalyst. An application of fluorinated JosiPhos ligands in ionic liquids was demonstrated using (S_p,*R*)-**288**, *i.e.*, the imidazolium-based analogue of (S_p,*R*)-**286**, in combination with [Rh(norbornadiene)$_2$]BF_4.[107b] The asymmetric hydrogenation reaction of methyl acetamidoacrylate, run under biphasic *tert*-butyl methyl ether/[bmim]BF_4 conditions, afforded the corresponding product with 99% ee using either (S_p,*R*)-**286** or (S_p,*R*)-**288**. More importantly, the ionic tag on (S_p,*R*)-**288** allows better recyclability of the fluorinated catalyst in the chosen co-solvent system. Chiral thiourea-derived diphosphine ligand (R_p,*S*)-**289** was used in the Rh^I-catalyzed hydrogenation

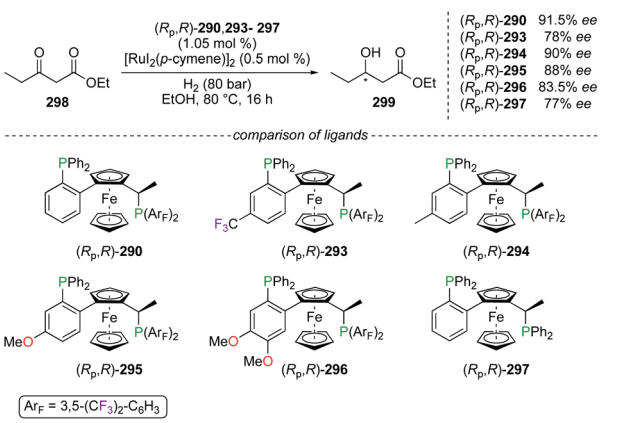

Scheme 33 Hydrogenation reaction using electronically modified WalPhos ligands.

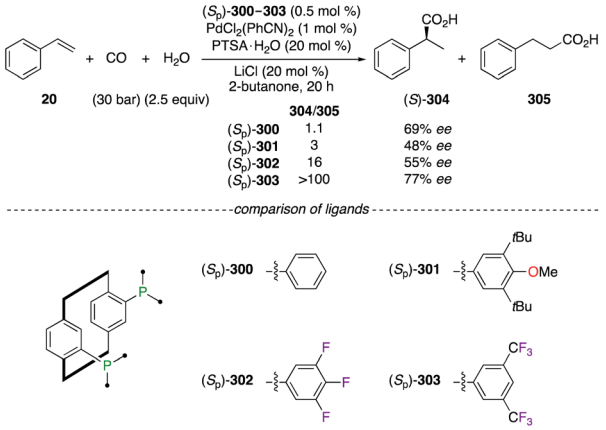

Scheme 34 Pd^{II}-Catalyzed carbonylation reaction of styrene **20**.

reactions,[108] where synergetic dual catalysis was induced by both the P_2 ligated Lewis acid and the Brønsted acid. Control experiments revealed an important gain of ee when a stronger hydrogen bonding was provided by the thiourea moiety. WalPhos-type diphosphines (R_p,*R*)-**290–292** were also described as a promising class of ligands in Rh^{I}, Ru^{II}, and Cu^{I} catalysis.[109]

Other fluorinated WalPhos-type diphosphines ligands (R_p,*R*)-**293–296** were designed to incorporate various electronic substituents on the aromatic backbone, not directly at the P atom. Such fine-tuning of the chiral ligand was studied in the Ru^{II}-catalyzed hydrogenation of ethyl 3-oxopentanoate **298** into **299** (Scheme 33).[109b] Unfortunately, no significant improvement of the chiral induction, arising from the electronic modifications of (R_p,*R*)-**293–296**, was demonstrated in comparison with the results obtained using ligands (R_p,*R*)-**290** and (R_p,*R*)-**297** as references. Noteworthily, conformational structures of chiral Ru^{II} complexes, obtained from (R_p,*R*)-**293**, (R_p,*R*)-**296**, and (R_p,*R*)-**297**, were investigated through XRD analysis.

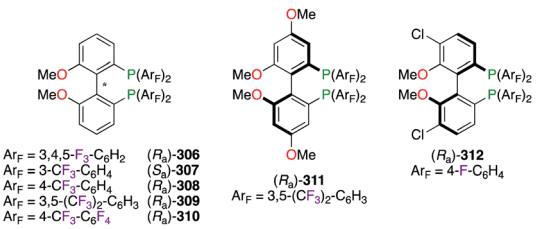

Fig. 15 F-Containing MeO-BIPHEP derivatives.

Planar chirality was further exploited in the hydroxycarbonylation reaction of styrene **20** using PhanePhos ligands (S_p)-**300–303**, all being available either in their S_p or R_p enantiomeric forms (Scheme 34). Chiral dinuclear Pd^{II} catalysts made from fluorinated ligands (S_p)-**302** and (S_p)-**303** afforded an increased selectivity for the branched regioisomer (*S*)-**304** *vs.* the selectivity obtained using the electron-rich PhanePhos ligands (S_p)-**300** and (S_p)-**301**. Moreover, the highest ee was achieved using the (S_p)-**303**/Pd^{II}_2 catalytic system.[110]

2.5.2 Axially chiral diphosphines. A Pd^{II}-catalyzed P–C coupling reaction,[111] between enantiomerically enriched phosphanes and aryl iodides, inspired the synthesis of a wide library of F-containing atropisomeric 2,2′-bis(diphenylphosphino)-6,6′-dimethoxy-1,1′-biphenyl (MeO-BIPHEP) ligands **306–312** (Fig. 15). The development of polyfluorinated MeO-BIPHEP derivatives, comprising F_{12}-((R_a)-**306**,[112] (S_a)-**307**,[113] (R_a)-**308**),[113,114] F_{24}-((R_a)-**309**)[114,115] and F_{28}-analogues ((R_a)-**310**),[112a] was undertaken, and these ligands were used as the chiral source for a variety of enantioselective transformations. Electronic modifications to the diaryl-core were explored for methoxy- or chlorine-substitutions at the 4,4′- and 5,5′-positions giving (R_a)-**311** [116] – commercialized as (*R*)-BTFM-GarPhos™ – and (R_a)-**312**,[117] respectively.

The family of axially chiral F-containing bisphosphine ligands was extended to achieve a priority objective, where the fine-tuning of the dihedral angle between the two aromatic rings was targeted (Fig. 16). Ligand design targeting structural variations arising from steric or electronic interactions, for getting optimum stereoselectivities, were extensively explored. Accordingly, all ligands were classified based on the 1,1′-biphenyl backbone: (i) BIPHEP-((S_a)-**313** and (S_a)-**314**),[118] (ii) DifluorPhos-((R_a)-**315**),[106a,119] (iii) SynPhos-((R_a)-**316** and (R_a)-**317**),[120] (iv) C_3-TunePhos-((R_a,*S*,*S*)-**318** and (S_a,*R*,*R*)-**319**),[121] (v) BIFUP- or FUPMOP-((S_a)-**320** and (S_a)-**321**),[122] and (vi) 2,2′-bis(-diphenylphosphino)-1,1′-binaphthyl (BINAP)-type of ligands (**322–324**).[119b,123] Based on comparative studies toward five

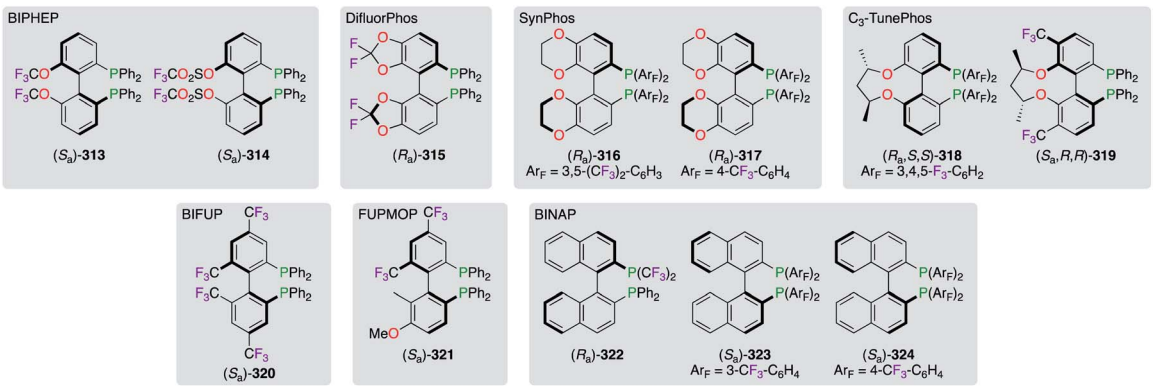

Fig. 16 Classes of axially chiral bisphosphine ligands comprising the 1,1′-biphenyl system.

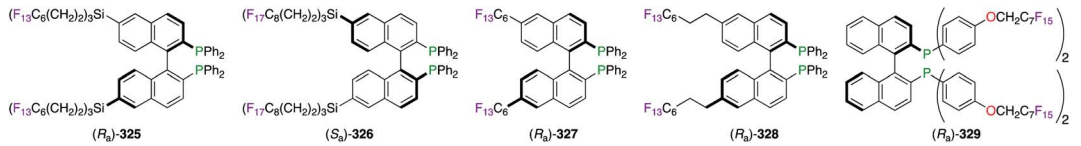

Fig. 17 Fluorous BINAPs employed in FBS.

selected classes of ligands, the narrowest dihedral angle was attributed to DifluorPhos-type ligands ($\theta \sim 67°$), whereas BINAP derivatives ($\theta \sim 86°$) were located at the other end of the steric scale.[119a,b] Overall, all electronically impoverished ligands, with specific steric profiles, showed excellent chiral inductions when complexed with the appropriate Lewis acid in various asymmetric reactions.

Strategies towards the recycling of the chiral ligand have encouraged the derivatization of BINAPs to incorporate perfluoroalkyl chains within their skeleton (Fig. 17). Fluorine substitution upon the naphthyl-backbone was then chosen for the synthesis of (R_a)-**325**. The asymmetric Heck reaction of 2,3-dihydrofuran was successfully performed in the benzene/FC-72 system using (R_a)-**325**/Pd^{II}.[28b,124] The Ru^{II}-catalyzed hydrogenation reaction of dimethyl itaconate was described using heavier fluorinated BINAP (S_a)-**326**, which was immobilized on fluorous silica gel.[125] Excellent retention of the fluorous ligand within the silica pores, *via* noncovalent interactions with the C_8F_{17} chains, permitted its recycling without the use of conventional biphasic extraction methods. Similar to (R_a)-**325**, F-containing BINAPs (R_a)-**327** and (R_a)-**328** were developed for their great ability as "light" fluorous ligands to be extracted from the other organic compounds *via* simple FRP column chromatography.[126] Introducing the perfluoroalkyl chain at the P atom, as highlighted by (R_a)-**329**, afforded poor ees in three metal-catalyzed reactions potentially due to the proximity of the fluorous tails to the activating site.[127] The relatively low fluorine content of (R_a)-**329** (51.5%) failed to give satisfactory chiral inductions in FBS. However, (R_a)-**329** was separated from the reaction mixture quickly using liquid–liquid extraction by perfluorocarbons.

Research towards the development of greener synthetic methods focused on the replacement of commonly used organic solvents by less hazardous and more environmentally benign alternatives, *e.g.*, supercritical carbon dioxide ($scCO_2$). The Rh^I-catalyzed hydroformylation reaction of monosubstituted alkenes **20**, **331–333** was performed in supercritical fluids using phosphine–phosphite BINAPHOS (R_a,S_a)-**330** (Scheme 35).[128] The aldehydes **334–337** were obtained with good regioselectivities and enantioselectivities using the (R_a,S_a)-**330**/Rh^I catalytic system. Considered as CO_2-philic, the perfluoralkyl chains permitted sufficient solubility of the ligand to be used under homogeneous reaction conditions. Moreover, C_4F_9, C_6F_{13}, and C_8F_{17} ponytails were incorporated into the 1,1′-binaphthyl core to generate $[R_F(CH_2)_3]$–BINAPHOS analogues.[129]

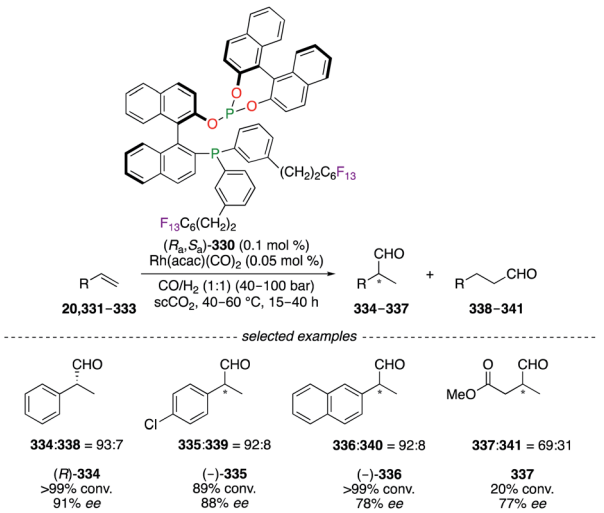

Scheme 35 (R_a,S_a)-**330**/Rh^I-Catalyzed hydroformylation reaction of alkenes.

2.5.3 Phosphoramidites. A wide library of monodentate phosphoramidite ligands was designed for numerous metal-catalyzed asymmetric reactions (Fig. 18).[130] Following the long-arm approach, substituted phenyl rings were incorporated at the 3,3′-positions of the binaphthol skeleton in order to enhance chiral inductions. Indeed, the space surrounding the ligated metal centre was considerably restricted by bulky 3,5-$(CF_3)_2$ and 4-NO_2 aromatic rings, as observed in (S_a)-**342**/(R_a)-**343** and (S_a)-**344**/(R_a)-**345**, respectively. An additional fine-tuning of the chiral ligands was possible at the amine moiety,

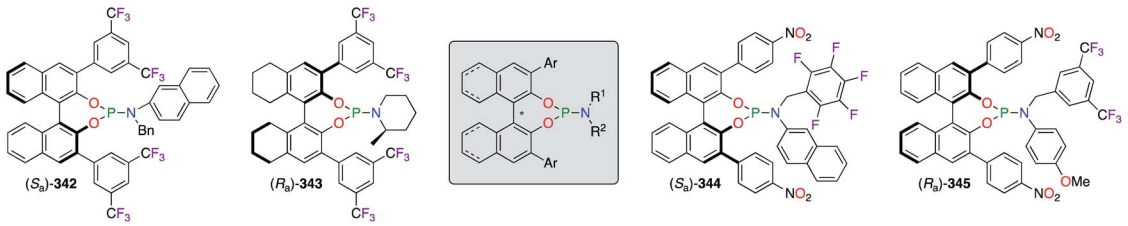

Fig. 18 Selected examples of chiral phosphoramidite ligands.

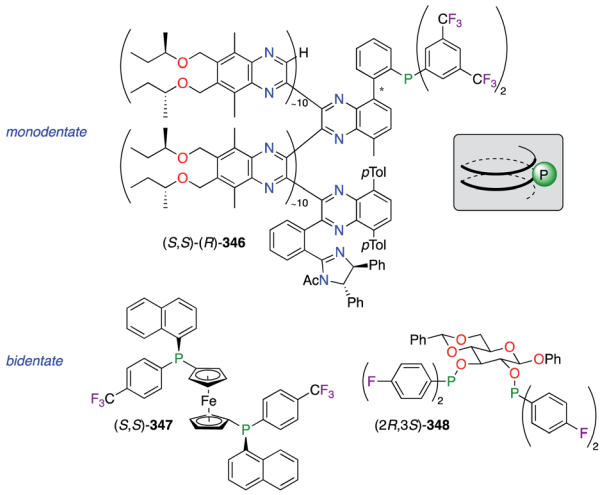

Fig. 19 Miscellaneous mono- and bidentate *P*-ligands containing fluorine atoms.

where electron-deficient benzyl substituents ((*S*$_a$)-**344**/(*R*$_a$)-**345**) or hindered piperidine ((*R*$_a$)-**343**) were generally more beneficial as observed from the obtained ees. A set of (*R*,*R*)-TADDOL-derived phosphoramidite ligands were screened in the Pd^{II}/Cu^{I}-catalyzed alkynylation reaction, but only the aryl substituents bearing bulky TMS groups and one electron withdrawing F atom afforded the optimal chiral induction.[131]

(*R*)-BINOL-based phosphite ligands, generated from 3,5-bis(trifluoromethyl)phenol and 2,2,2-trifluoroethanol, were considered as promising ligands in the synthesis of Rh^{I} complexes and their use in enantioselective catalysis in ionic liquids.[132]

2.5.4 Other P ligands. Fluorinated monophosphine, stereogenic phosphine, and sugar-derived phophinite ligands have been complexed with various noble metals (Fig. 19). The (10–1–10) copolymer poly(quinoxaline-2,3-diyl)phosphine (PQXphos) (*S*,*S*)–(*R*)-**346**, having *P* helicity, was employed as a screened ligand in the asymmetric Pd^{0}-catalyzed Suzuki–Miyaura coupling reaction, giving only a moderate chiral induction.[133] Interestingly, the sense of the chirality (*R*$_a$ or *S*$_a$) at the active site of **346** would be induced, according to the structure models,[133b] by the helicity adopted by the polymer either in the right-handed (*P*) or the left-handed (*M*) helix geometry, respectively. Another monodentate (1*R*,3*R*,4*S*)-menthyl-based phosphine ligand, bearing two C_6F_{13} and C_8F_{17} ponytails, was reported to give fluorous chiral catalysts when mixed with Ir^{I} and Rh^{I} salts.[134] Chiral at P atoms, diphosphine ligand (*S*,*S*)-**347**, belonging to the class of 1,1′-bis(diphenylphosphino)ferrocenes (dppf), was designed to modulate the stereoselective event in the Pd^{II}-catalyzed nucleophilic substitution of allylic acetates.[135] When *rac*-**114** and **115** were used as substrates, the combination of the bulky 1-naphthyl substituent with the electronically deficient 4-F-C_6H_4 unit afforded a slightly lower enantioselectivity (61% ee of (*S*)-**116**) than the unfluorinated one (68% ee of (*R*)-**116**) and its electron donating analogue (4-OMe-C_6H_4; 69% ee of (*S*)-**116**). A Pt^{II}-catalyzed alkylation of linked secondary phosphines (HRP–PRH) in the presence of various benzyl bromides, comprising F- and CF_3-containing ones, led to *P*-stereogenic diphosphines with low stereoselectivities.[136] The hydrogenation of a variety dehydroamino acids was reported using chiral phosphinite/Rh^{I} catalysts made from various carbohydrate scaffolds.[137] Being highly dependent on the *P*-aryl substituent, the level of chiral induction was demonstrated to be considerably higher when using electron-rich bis(3,5-dimethylphenyl) groups *vs.* electron-poor ones, such as C2,C3-bis-(di-4-fluorophenyl)phosphinite ligand (2*R*,3*S*)-**348**, derived from phenyl β-D-glucopyranoside. Furthermore, a (*R*,*R*)-DIOP-like 4-(trifluoromethyl)phenylboronate diphosphine ligand was synthesized and mixed with Rh^{I}, Pd^{II}, and Pt^{II} salts to generate heterobimetallic complexes.[138]

In general, the 3,5-$(CF_3)_2$-C_6H_3 substituent has been widely used in *P*-based chiral ligands. Various fluorous ponytails were incorporated into BINAP ligands to give "heavy" and "light" fluorous analogues to be used in distinct synthetic applications. Major advancements were demonstrated using CO_2-philic BINAPHOS ligands bearing perfluoroalkyl chains, in the enantioselective hydroformylation reaction performed in supercritical carbon dioxide. Noteworthily, this section has detailed numerous mono- and diphosphines incorporating a large range of structurally diverse fluorine containing groups.

2.6 *P*,*O*-Based binding modes

Being *O*-alkylated with perfluoroalkyl chains at the very last step of the synthesis, 2-(diphenylphosphino)-2′-alkoxy-1,1′-binaphthyl (MOP) (*R*$_a$)-**349** was used, together with [Pd(η^3-C_3H_5)Cl]$_2$, in the asymmetric alkylation reaction of β-dicarbonyl derivatives with 1,3-diphenyl-2-propenyl *rac*-**114** (Scheme 36).[127,139] The corresponding alkylated products (*R*)-**116** and **353–355** were obtained in moderate to excellent yields, and good ees were obtained. Noteworthily, (*R*$_a$)-**349** was completely extracted from the reaction mixture using *n*-perfluorooctane, whereas the catalytic activity of the recycled Pd^{II} complex was lost when used in subsequent reactions.

2.7 *C*-Based binding modes

2.7.1 Diaminocarbenes. Chiral Au^{I} complexes (*R*$_a$)-**356–358** involving acyclic diaminocarbene ligands were described as efficient catalysts in the cyclization reaction of

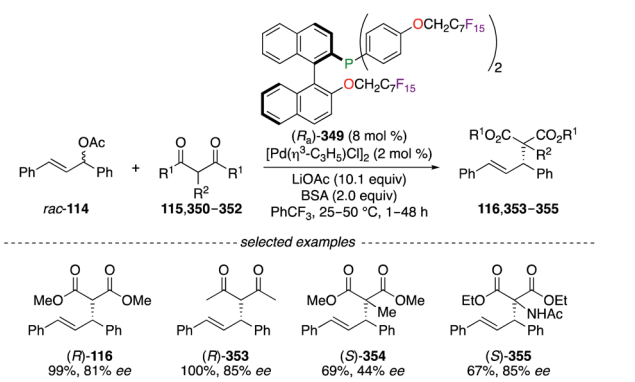

Scheme 36 (*R*$_a$)-**349**/Pd^{II}-catalyzed alkylation reaction of *rac*-**114**.

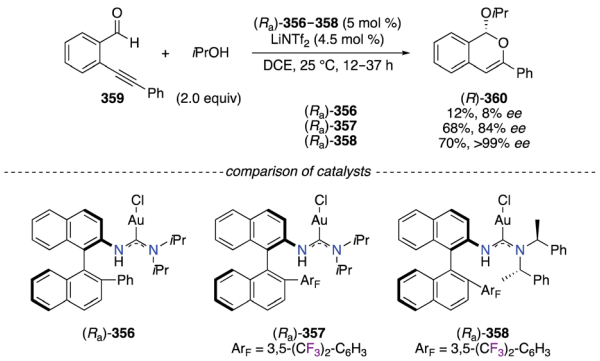

Scheme 37 Au^{I}-Catalyzed cyclization of **359** into (*R*)-**360**.

alkynylbenzaldehyde **359** and ^{i}PrOH (Scheme 37).[140] Cycloadduct (*R*)-**360** was obtained in various levels of enantioselectivity depending on the presence of the 3,5-$(CF_3)_2$-C_6H_3 group on the adjacent naphthyl ring ((*R*$_a$)-**357** and (*R*$_a$)-**358** *vs.* (*R*$_a$)-**356**). As revealed by XRD and DFT studies, strong Au^{I}–π interactions with the electron-deficient F-arene give an increased stability to the catalyst, by limiting the number of possible rotamers, therefore locating the chiral environment in the optimal orientation. Bulkier substituents at the amine moiety ((*S*)-PhMeCH *vs.* ^{i}Pr) further enhanced steric interactions around the Au^{I} centre and thus the obtained enantioselectivity.

N-heterocyclic carbene (NHC)–Cu^{I} catalysts (*S*,*S*)-**361–363** were employed in the asymmetric allylic arylation (AAAr) of aliphatic allylic bromides **364–366** with PhMgBr (Scheme 38).[141] Overall, the substitution by sterically hindered and electron-deficient aryl groups onto chiral NHC–Cu^{I} complexes, *e.g.*, (*S*,*S*)-**362** and (*S*,*S*)-**363**, was found beneficial to obtain a higher regioselectivity towards the γ-regioisomers **367–369** than (*S*,*S*)-**361**. When using the allylic bromide **364**, the best enantioselectivity was afforded by using (*S*,*S*)-**361**, but sterically and electronically fine-tuned catalysts considerably improved the γ-selectivity (**367** : **370** up to 92 : 8). Excellent regioselectivity for (*R*)-**368** was obtained particularly with (*S*,*S*)-**362**, whereas excellent enantioselectivities were rather observed when using (*S*,*S*)-**361** and (*S*,*S*)-**363**. The NHC–Cu^{I}-catalyzed AAAr of **366** led to α-product **372** preferentially, and only the F-containing catalyst

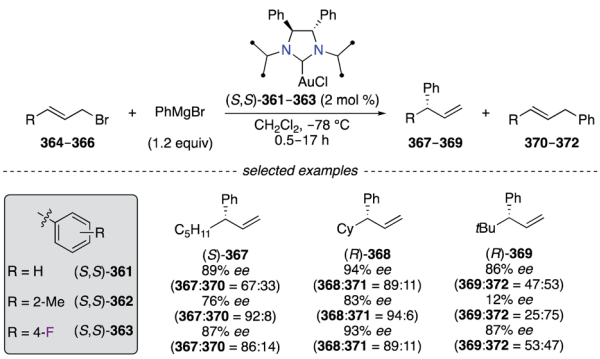

Scheme 38 NHC–Cu^{I}-Catalyzed AAAr reaction of aliphatic allylic bromides with phenyl magnesium bromide.

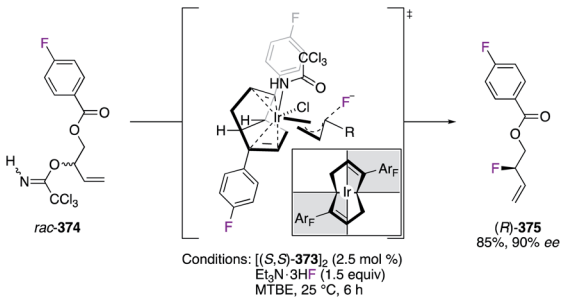

Scheme 39 Fluorination reaction *via* the optimized TS.

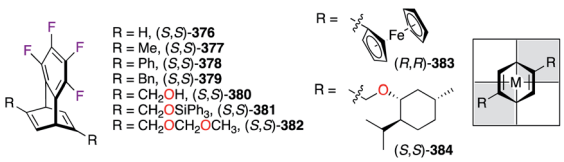

Fig. 20 Chiral tfb-substituted ligands and their complexation modes with metals.

(*S*,*S*)-**363** afforded (*R*)-**369** with the best regio- and enantioselectivity when using a sterically hindered ^{t}Bu-substrate.

2.7.2 Dienes. The fluorination reaction of allylic trichloroacetimidates *rac*-**374** was performed *via* a dynamic kinetic asymmetric transformation (DKAT) mechanism using the Ir^{I} pre-catalyst [(*S*,*S*)-**373**]$_2$ (Scheme 39).[142] Chelated by the fluorinated (*S*,*S*)-bicyclo[3.3.0]octadiene ligand, the Ir^{I} centre generated, *via* ionization of the substrate, the lowest energetically π-allyl intermediate of the computed diastereomeric TSs. Accordingly, the most substituted carbon undergoes nucleophilic attack of the fluoride from the outer-sphere, and (*R*)-**375** was obtained with excellent regio- and enantioselectivities.

Rh^{I}- or Ir^{I}-catalyzed highly enantioselective organic transformations, *i.e.*, arylation,[143] conjugate addition,[144] and cyclization reactions,[145] were demonstrated using C_2-symmetric tetrafluorobenzobarrelene (tfb) ligands **376–384** (Fig. 20). The bicyclic [2.2.2]octatriene skeleton was obtained in both *R*,*R* and *S*,*S* enantiomeric forms *via* the resolution of the racemic mixture by high pressure chiral liquid chromatography. Once the desired arms attached, the electronically deficient diene ligands **376–384** strongly chelate metal cations, and high sterically hindered environments are then created in the upper right and lower left quadrants.[146]

3. Conclusions

The introduction of the fluorine atom has revealed a positive modulation of stereoselective events using metal catalysis. An optimal balance between an ideal substrate activation and an inherent stability of the catalyst can be established by using these electron-deficient ligands. The examples presented herein demonstrate that the fluorine atom fine-tunes both electronic and steric properties of the chiral catalyst. The high availability of F-containing aromatic compounds, particularly bearing the 3,5-$(CF_3)_2$-C_6H_3 and the 4-CF_3-C_6H_4 motifs, favours their

incorporation into desired specific positions. Generally, their high electron withdrawing ability was exploited for reaching increased acidity of the chelated Lewis acid. Also, the chiral environments were often better defined by the participation of the fluorinated aromatic ring through electrostatic pairing, both with the metal centre in the inner sphere and the substrate orientation in the outer sphere. The use of the fluorine atom and polyfluorinated groups as a steric bulk remains underdeveloped in asymmetric catalysis. Unexpected high chiral inductions, which are scarcely reported in the literature, are likely to arise from the intrinsic steric properties of bulky polyfluorinated substituents. Besides stereoelectronic reasons, the presence of fluorine in chiral ligands is also valuable from a green chemistry perspective. The fluorophilic effect, which is observed in the presence of perfluoroalkyl chains, has indeed opened the field of asymmetric catalysis into fluorous biphasic systems. Due to easy extraction procedures, many advantages were highlighted by the recycling of the chiral catalyst over multiple runs without the loss of chiral induction over time. Not only is the fluorine atom considered as a highly multifunctional tool for ligand design, but also its judicious employment is of paramount importance for metal-catalyzed asymmetric transformations.

Author contributions

The manuscript was written through contributions of all authors. All authors have given approval to the final version of the manuscript.

Conflicts of interest

There are no conflicts to declare.

Acknowledgements

This work was supported by the Natural Sciences and Engineering Research Council of Canada (NSERC) Discovery Grant RGPIN-2017-04272, the FRQNT Centre in Green Chemistry and Catalysis (CGCC) Strategic Cluster FRQNT-2020-RS4-265155-CCVC, and Université Laval (UL). S. L. thanks NSERC and FRQNT for graduate scholarships.

Notes and references

1 (*a*) K. Seppelt, *The Curious World of Fluorinated Molecules: Molecules Containing Fluorine*, Elsevier, Amsterdam, 2021; (*b*) A. Tressaud, *Fluorine: A Paradoxal Element*, Elsevier, Amsterdam, 2019; (*c*) P. Kirsch, *Modern Fluoroorganic Chemistry: Synthesis, Reactivity, Applications*, Weinheim, 2013.

2 D. O'Hagan and D. B. Harper, *J. Fluorine Chem.*, 1999, **100**, 127–133.

3 (*a*) H. Mei, J. Han, S. Fustero, M. Medio-Simon, D. M. Sedgwick, C. Santi, R. Ruzziconi and V. A. Soloshonok, *Chem.–Eur. J.*, 2019, **25**, 11797–11819; (*b*) Y. Zhou, J. Wang, Z. Gu, S. Wang, W. Zhu, J. L. Aceña, V. A. Soloshonok, K. Izawa and H. Liu, *Chem. Rev.*, 2016, **116**, 422–518; (*c*) J. Wang, M. Sánchez-Roselló, J. L. Aceña, C. del Pozo, A. E. Sorochinsky, S. Fustero, V. A. Soloshonok and H. Liu, *Chem. Rev.*, 2014, **114**, 2432–2506.

4 (*a*) N. A. Meanwell, *J. Med. Chem.*, 2018, **61**, 5822–5880; (*b*) E. P. Gillis, K. J. Eastman, M. D. Hill, D. J. Donnelly and N. A. Meanwell, *J. Med. Chem.*, 2015, **58**, 8315–8359; (*c*) W. K. Hagmann, *J. Med. Chem.*, 2008, **51**, 4359–4369; (*d*) S. Purser, P. R. Moore, S. Swallow and V. Gouverneur, *Chem. Soc. Rev.*, 2008, **37**, 320–330; (*e*) K. Müller, C. Faeh and F. Diederich, *Science*, 2007, **317**, 1881–1886.

5 D. O'Hagan, *Chem. Soc. Rev.*, 2008, **37**, 308–319.

6 (*a*) D. Cahard and V. Bizet, *Chem. Soc. Rev.*, 2014, **43**, 135–147; (*b*) F. Fache, *New J. Chem.*, 2004, **28**, 1277–1283; (*c*) G. Pozzi and I. Shepperson, *Coord. Chem. Rev.*, 2003, **242**, 115–124; (*d*) L. E. Zimmer, C. Sparr and R. Gilmour, *Angew. Chem. Int. Ed.*, 2011, **50**, 11860–11871.

7 M. Stradiotto and R. J. Lundgren, *Ligand Design in Metal Chemistry: Reactivity and Catalysis*, Chichester, 2016.

8 (*a*) A. L. Allred, *J. Inorg. Nucl. Chem.*, 1961, **17**, 215–221; (*b*) P. R. Wells, in *Progress in Physical Organic Chemistry*, ed. A. Streitwieser Jr and R. W. Taft, John Wiley & Sons, New York, 1968, vol. 6, pp. 111–145; (*c*) J. E. Huheey, *J. Phys. Chem.*, 1965, **69**, 3284–3291; (*d*) J. Hinze, M. A. Whitehead and H. H. Jaffé, *J. Am. Chem. Soc.*, 1963, **85**, 148–154.

9 (*a*) J. A. Hirsch, in *Topics in Stereochemistry*, ed. N. Allinger and E. L. Eliel, John Wiley & Sons, New York, 1967, vol. 1, pp. 199−222; (*b*) E. L. Eliel, S. H. Wilen and L. N. Mander, *Stereochemistry of Organic Compounds*, John Wiley & Sons, New York, 1994; (*c*) Y. Carcenac, M. Tordeux, C. Wakselman and P. Diter, *New J. Chem.*, 2006, **30**, 447–457.

10 S. H. Unger and C. Hansch, in *Progress in Physical Organic Chemistry*, ed. R. W. Taft, John Wiley & Sons, New York, 1976, vol. 12, pp. 91–118.

11 (*a*) M. Charton, *J. Am. Chem. Soc.*, 1975, **97**, 1552–1556; (*b*) M. Charton, *J. Org. Chem.*, 1976, **41**, 2217–2220.

12 G. Bott, L. D. Field and S. Sternhell, *J. Am. Chem. Soc.*, 1980, **102**, 5618–5626.

13 A. V. Brethomé, S. P. Fletcher and R. S. Paton, *ACS Catal.*, 2019, **9**, 2313–2323.

14 A. Bondi, *J. Phys. Chem.*, 1964, **68**, 441–451.

15 (*a*) J. A. Gladysz, D. P. Curran and I. T. Horváth, *Handbook of Fluorous Chemistry*, Wiley-VCH, Weinheim, 2004; (*b*) K. Mikami, *Green Reaction Media in Organic Synthesis*, Blackwell Publishing, Oxford, 2005.

16 S. Suzuki, H. Furuno, Y. Yokoyama and J. Inanaga, *Tetrahedron: Asymmetry*, 2006, **17**, 504–507.

17 J.-S. Lin, F.-L. Wang, X.-Y. Dong, W.-W. He, Y. Yuan, S. Chen and X.-Y. Liu, *Nat. Commun.*, 2017, **8**, 1–11.

18 T. Li, P. Yu, Y.-M. Du, J.-S. Lin, Y. Zhi and X.-Y. Liu, *J. Fluorine Chem.*, 2017, **203**, 210–214.

19 J. Lv, L. Zhang, S. Hu, J.-P. Cheng and S. Luo, *Chem.–Eur. J.*, 2012, **18**, 799–803.

20 A. Biffis, M. Braga, S. Cadamuro, C. Tubaro and M. Basato, *Org. Lett.*, 2005, **7**, 1841–1844.

21 F. Yang, D. Zhao, J. Lan, P. Xi, L. Yang, S. Xiang and J. You, *Angew. Chem. Int. Ed.*, 2008, **47**, 5646–5649.
22 M. Ogasawara, S. Watanabe, K. Nakajima and T. Takahashi, *J. Am. Chem. Soc.*, 2010, **132**, 2136–2137.
23 S. Superchi, M. I. Donnoli and C. Rosini, *Tetrahedron Lett.*, 1998, **39**, 8541–8544.
24 L. J. P. Martyn, S. Pandiaraju and A. K. Yudin, *J. Organomet. Chem.*, 2000, **603**, 98–104.
25 (*a*) Q.-L. Zhou, *Privileged Chiral Ligands and Catalysts*, Wiley-VCH, Weinheim, 2011; (*b*) T. P. Yoon and E. N. Jacobsen, *Science*, 2003, **299**, 1691–1693.
26 (*a*) Y. S. Sokeirik, A. Hoshina, M. Omote, K. Sato, A. Tarui, I. Kumadaki and A. Ando, *Chem.–Asian J.*, 2008, **3**, 1850–1856; (*b*) Y. S. Sokeirik, H. Mori, M. Omote, K. Sato, A. Tarui, I. Kumadaki and A. Ando, *Org. Lett.*, 2007, **9**, 1927–1929.
27 W.-S. Huang and L. Pu, *Tetrahedron Lett.*, 2000, **41**, 145–149.
28 (*a*) Y. Nakamura, S. Takeuchi, K. Okumura, Y. Ohgo and D. P. Curran, *Tetrahedron*, 2002, **58**, 3963–3969; (*b*) Y. Nakamura, S. Takeuchi and Y. Ohgo, *J. Fluorine Chem.*, 2003, **120**, 121–129; (*c*) Y. Tian, Q. C. Yang, T. C. W. Mak and K. S. Chan, *Tetrahedron*, 2002, **58**, 3951–3961; (*d*) Y. Nakamura, S. Takeuchi, Y. Ohgo and D. P. Curran, *Tetrahedron Lett.*, 2000, **41**, 57–60.
29 Y. Tian and K. S. Chan, *Tetrahedron Lett.*, 2000, **41**, 8813–8816.
30 Y. Nakamura, S. Takeuchi, Y. Ohgo and D. P. Curran, *Tetrahedron*, 2000, **56**, 351–356.
31 C. Wang, X. Wu and L. Pu, *Chem.–Eur. J.*, 2017, **23**, 10749–10752.
32 (*a*) M. Omote, Y. Nishimura, K. Sato, A. Ando and I. Kumadaki, *Tetrahedron*, 2006, **62**, 1886–1894; (*b*) M. Omote, Y. Nishimura, K. Sato, A. Ando and I. Kumadaki, *Tetrahedron Lett.*, 2005, **46**, 319–322; (*c*) M. Omote, T. Hasegawa, K. Sato, A. Ando and I. Kumadaki, *Heterocycles*, 2003, **59**, 501–504; (*d*) M. Omote, A. Kominato, M. Sugawara, K. Sato, A. Ando and I. Kumadaki, *Tetrahedron Lett.*, 1999, **40**, 5583–5585.
33 (*a*) M. Omote, N. Tanaka, A. Tarui, K. Sato, I. Kumadaki and A. Ando, *Tetrahedron Lett.*, 2007, **48**, 2989–2991; (*b*) M. Omote, Y. Nishimura, K. Sato, A. Ando and I. Kumadaki, *J. Fluorine Chem.*, 2005, **126**, 407–409; (*c*) M. Omote, Y. Nishimura, K. Sato, A. Ando and I. Kumadaki, *J. Fluorine Chem.*, 2006, **127**, 74–78.
34 S. Lauzon and T. Ollevier, *Chem. Commun.*, 2021, **57**, 11025–11028.
35 Y. S. Sokeirik, M. Omote, K. Sato, I. Kumadaki and A. Ando, *Tetrahedron: Asymmetry*, 2006, **17**, 2654–2658.
36 (*a*) T. Katagiri, Y. Fujiwara, S. Takahashi, N. Ozaki and K. Uneyama, *Chem. Commun.*, 2002, 986–987; (*b*) A. Harada, Y. Fujiwara and T. Katagiri, *Tetrahedron: Asymmetry*, 2008, **19**, 1210–1214.
37 Y. Fujiwara, T. Katagiri and K. Uneyama, *Tetrahedron Lett.*, 2003, **44**, 6161–6163.
38 G. Zhao, X.-G. Li and X.-R. Wang, *Tetrahedron: Asymmetry*, 2001, **12**, 399–403.
39 J. K. Park, H. G. Lee, C. Bolm and B. M. Kim, *Chem.–Eur. J.*, 2005, **11**, 945–950.
40 Y.-Z. Liu, S.-J. Shang, W.-L. Yang, X. Luo and W.-P. Deng, *J. Org. Chem.*, 2017, **82**, 11141–11149.
41 K. Li, X. Sun, L. Li, Z. Zha, F.-L. Zhang and Z. Wang, *Chem.–Eur. J.*, 2021, **27**, 581–584.
42 B. M. Trost, V. S. C. Yeh, H. Ito and N. Bremeyer, *Org. Lett.*, 2002, **4**, 2621–2623.
43 A. M. Cook and C. Wolf, *Angew. Chem. Int. Ed.*, 2016, **55**, 2929–2933.
44 Y. Yi, Y.-Z. Hua, H.-J. Lu, L.-T. Liu and M.-C. Wang, *Org. Lett.*, 2020, **22**, 2527–2531.
45 J. A. Sehnem, P. Milani, V. Nascimento, L. H. Andrade, L. Dorneles and A. L. Braga, *Tetrahedron: Asymmetry*, 2010, **21**, 997–1003.
46 (*a*) M. Cavazzini, A. Manfredi, F. Montanari, S. Quici and G. Pozzi, *Eur. J. Org. Chem.*, 2001, 4639–4649; (*b*) M. Cavazzini, A. Manfredi, F. Montanari, S. Quici and G. Pozzi, *Chem. Commun.*, 2000, 2171–2172; (*c*) G. Pozzi, M. Cavazzini, F. Cinato, F. Montanari and S. Quici, *Eur. J. Org. Chem.*, 1999, 1947–1955; (*d*) G. Pozzi, F. Cinato, F. Montanari and S. Quici, *Chem. Commun.*, 1998, 877–878.
47 (*a*) M. Cavazzini, S. Quici and G. Pozzi, *Tetrahedron*, 2002, **58**, 3943–3949; (*b*) I. Shepperson, M. Cavazzini, G. Pozzi and S. Quici, *J. Fluorine Chem.*, 2004, **125**, 175–180.
48 D. Maillard, G. Pozzi, S. Quici and D. Sinou, *Tetrahedron*, 2002, **58**, 3971–3976.
49 Y. Kobayashi, R. Obayashi, Y. Watanabe, H. Miyazaki, I. Miyata, Y. Suzuki, Y. Yoshida, T. Shioiri and M. Matsugi, *Eur. J. Org. Chem.*, 2019, 2401–2408.
50 (*a*) E. Kirillov, L. Lavanant, C. Thomas, T. Roisnel, Y. Chi and J.-F. Carpentier, *Chem.–Eur. J.*, 2007, **13**, 923–935; (*b*) L. Lavanant, T.-Y. Chou, Y. Chi, C. W. Lehmann, L. Toupet and J.-F. Carpentier, *Organometallics*, 2004, **23**, 5450–5458; (*c*) T. Tsukahara, D. C. Swenson and R. F. Jordan, *Organometallics*, 1997, **16**, 3303–3313.
51 M. P. Doyle, W. Hu, I. M. Phillips, C. J. Moody, A. G. Pepper and A. M. Z. Slawin, *Adv. Synth. Catal.*, 2001, **343**, 112–117.
52 T. Remarchuk and E. J. Corey, *Tetrahedron Lett.*, 2018, **59**, 2256–2259.
53 (*a*) Z. Li, K. R. Conser and E. N. Jacobsen, *J. Am. Chem. Soc.*, 1993, **115**, 5326–5327; (*b*) Z. Li, R. W. Quan and E. N. Jacobsen, *J. Am. Chem. Soc.*, 1995, **117**, 5889–5890; (*c*) L. A. Dakin, S. E. Schaus, E. N. Jacobsen and J. S. Panek, *Tetrahedron Lett.*, 1998, **39**, 8947–8950.
54 D. A. Evans, T. Lectka and S. J. Miller, *Tetrahedron Lett.*, 1993, **34**, 7027–7030.
55 V. Carreras, C. Besnard, V. Gandon and T. Ollevier, *Org. Lett.*, 2019, **21**, 9094–9098.
56 (*a*) B. M. Trost, D. L. Van Vranken and C. Bingel, *J. Am. Chem. Soc.*, 1992, **114**, 9327–9343; (*b*) R. C. Verboom, B. J. Plietker and J.-E. Bäckvall, *J. Organomet. Chem.*, 2003, **687**, 508–517.
57 H. Tye, C. Eldred and M. Wills, *Tetrahedron Lett.*, 2002, **43**, 155–158.
58 V. Devannah, R. Sharma and D. A. Watson, *J. Am. Chem. Soc.*, 2019, **141**, 8436–8440.

59 J. Y. Mang, D. G. Kwon and D. Y. Kim, *J. Fluorine Chem.*, 2009, **130**, 259–262.
60 A. N. Reznikov, L. E. Kapranov, V. V. Ivankina, A. E. Sibiryakova, V. B. Rybakov and Y. N. Klimochkina, *Helv. Chim. Acta*, 2018, **101**, e1800170.
61 I. Shepperson, S. Quici, G. Pozzi, M. Nicoletti and D. O'Hagan, *Eur. J. Org. Chem.*, 2004, 4545–4551.
62 J. Bayardon, D. Maillard, G. Pozzi and D. Sinou, *Tetrahedron: Asymmetry*, 2004, **15**, 2633–2640.
63 J. Bayardon, D. Sinou, O. Holczknecht, L. Mercs and G. Pozzi, *Tetrahedron: Asymmetry*, 2005, **16**, 2319–2327.
64 H. Kim, Y. Nguyen, C. P.-H. Yen, L. Chagal, A. J. Lough, B. M. Kim and J. Chin, *J. Am. Chem. Soc.*, 2008, **130**, 12184–12191.
65 (*a*) C. M. Marson and R. C. Melling, *J. Org. Chem.*, 2005, **70**, 9771–9779; (*b*) C. M. Marson and R. C. Melling, *Chem. Commun.*, 1998, 1223–1224.
66 H. Liu, S. Liu, H. Zhou, Q. Liu and C. Wang, *RSC Adv.*, 2018, **8**, 14829–14832.
67 W. Ma, J. Zhang, C. Xu, F. Chen, Y.-M. He and Q.-H. Fan, *Angew. Chem. Int. Ed.*, 2016, **55**, 12891–12894.
68 (*a*) W.-W. Wang and Q.-R. Wang, *Chem. Commun.*, 2010, **46**, 4616–4618; (*b*) W.-W. Wang, Z.-M. Li, L. Su, Q.-R. Wang and Y.-L. Wu, *J. Mol. Catal. A: Chem.*, 2014, **387**, 92–102.
69 C. Xu, L. Zhang, C. Dong, J. Xu, Y. Pan, Y. Li, H. Zhang, H. Li, Z. Yu and L. Xu, *Adv. Synth. Catal.*, 2016, **358**, 567–572.
70 (*a*) B. He, P. Phansavath and V. Ratovelomanana-Vidal, *Org. Chem. Front.*, 2020, **7**, 975–979; (*b*) B. He, L.-S. Zheng, P. Phansavath and V. Ratovelomanana-Vidal, *ChemSusChem*, 2019, **12**, 3032–3036; (*c*) L.-S. Zheng, Q. Llopis, P.-G. Echeverria, C. Férard, G. Guillamot, P. Phansavath and V. Ratovelomanana-Vidal, *J. Org. Chem.*, 2017, **82**, 5607–5615; (*d*) L.-S. Zheng, C. Férard, P. Phansavath and V. Ratovelomanana-Vidal, *Chem. Commun.*, 2018, **54**, 283–286.
71 X.-T. Li, Q.-S. Gu, X.-Y. Dong, X. Meng and X.-Y. Liu, *Angew. Chem. Int. Ed.*, 2018, **57**, 7668–7672.
72 (*a*) Y. Kawashima, T. Ezawa, M. Yamamura, T. Harada, T. Noguchi, T. Miura and N. Imai, *Tetrahedron*, 2015, **71**, 8585–8592; (*b*) T. Miura, K. Itoh, Y. Yasaku, N. Koyata, Y. Murakami and N. Imai, *Tetrahedron Lett.*, 2008, **49**, 5813–5815; (*c*) N. Imai, K. Sakamoto, M. Maeda, K. Kouge, K. Yoshizane and J. Nokami, *Tetrahedron Lett.*, 1997, **38**, 1423–1426.
73 S. Nakamura, K. Hyodo, Y. Nakamura, N. Shibata and T. Toru, *Adv. Synth. Catal.*, 2008, **350**, 1443–1448.
74 J.-S. Poh, S. Makai, T. von Keutz, D. N. Tran, C. Battilocchio, P. Pasau and S. V. Ley, *Angew. Chem. Int. Ed.*, 2017, **56**, 1864–1868.
75 A. T. Parsons and J. S. Johnson, *J. Am. Chem. Soc.*, 2009, **131**, 3122–3123.
76 T. Fan, H.-C. Shen, Z.-Y. Han and L.-Z. Gong, *Chin. J. Chem.*, 2019, **37**, 226–232.
77 (*a*) S. Abbina and G. Du, *Organometallics*, 2012, **31**, 7394–7403; (*b*) R. Ma, J. Young, R. Promontorio, F. M. Dannheim, C. C. Pattillo and M. C. White, *J. Am. Chem. Soc.*, 2019, **141**, 9468–9473.
78 (*a*) J. Bayardon and D. Sinou, *Tetrahedron Lett.*, 2003, **44**, 1449–1451; (*b*) J. Bayardon and D. Sinou, *J. Org. Chem.*, 2004, **69**, 3121–3128.
79 J. Bayardon, O. Holczknecht, G. Pozzi and D. Sinou, *Tetrahedron: Asymmetry*, 2006, **17**, 1568–1572.
80 R. Kolodziuk, C. Goux-Henry and D. Sinou, *Tetrahedron: Asymmetry*, 2007, **18**, 2782–2786.
81 J. Bayardon and D. Sinou, *Tetrahedron: Asymmetry*, 2005, **16**, 2965–2972.
82 (*a*) T. Deng and C. Cai, *J. Fluorine Chem.*, 2013, **156**, 183–186; (*b*) T. Deng, H. Wang and C. Cai, *Eur. J. Org. Chem.*, 2014, **2014**, 7259–7264; (*c*) T. Deng, H. Wang and C. Cai, *J. Fluorine Chem.*, 2015, **169**, 72–77; (*d*) T. Deng, H. Wang and C. Cai, *Org. Biomol. Chem.*, 2014, **12**, 5843–5846.
83 M. Buchsteiner, L. Martinez-Rodriguez, P. Jerabek, I. Pozo, M. Patzer, N. Nöthling, C. W. Lehmann and A. Fürstner, *Chem.–Eur. J.*, 2020, **26**, 2509–2515.
84 R. Rasappan, T. Olbrich and O. Reiser, *Adv. Synth. Catal.*, 2009, **351**, 1961–1967.
85 B. Simonelli, S. Orlandi, M. Benaglia and G. Pozzi, *Eur. J. Org. Chem.*, 2004, 2669–2673.
86 R. Annunziata, M. Benaglia, M. Cinquini, F. Cozzi and G. Pozzi, *Eur. J. Org. Chem.*, 2003, 1191–1197.
87 K. Tani, D. C. Behenna, R. M. McFadden and B. M. Stoltz, *Org. Lett.*, 2007, **9**, 2529–2531.
88 (*a*) Y. Lu, E. L. Goldstein and B. M. Stoltz, *Org. Lett.*, 2018, **20**, 5657–5660; (*b*) S. E. Shockley, J. C. Hethcox and B. M. Stoltz, *Tetrahedron Lett.*, 2017, **58**, 3341–3343; (*c*) D. E. White, I. C. Stewart, R. H. Grubbs and B. M. Stoltz, *J. Am. Chem. Soc.*, 2008, **130**, 810–811; (*d*) N. T. McDougal, J. Streuff, H. Mukherjee, S. C. Virgil and B. M. Stoltz, *Tetrahedron Lett.*, 2010, **51**, 5550–5554.
89 Z. Hu, Y. Li, K. Liu and Q. Shen, *J. Org. Chem.*, 2012, **77**, 7957–7967.
90 (*a*) M. P. Carroll, H. Müller-Bunz and P. J. Guiry, *Chem. Commun.*, 2012, **48**, 11142–11144; (*b*) R. Doran, M. P. Carroll, R. Akula, B. F. Hogan, M. Martins, S. Fanning and P. J. Guiry, *Chem.–Eur. J.*, 2014, **20**, 15354–15359.
91 Z. Jiang, L. Hou, C. Ni, J. Chen, D. Wang and X. Tong, *Chem. Commun.*, 2017, **53**, 4270–4273.
92 P. B. Armstrong, E. A. Dembicer, A. J. DesBois, J. T. Fitzgerald, J. K. Gehrmann, N. C. Nelson, A. L. Noble and R. C. Bunt, *Organometallics*, 2012, **31**, 6933–6946.
93 B. Liu, Z.-M. Zhang, B. Xu, S. Xu, H.-H. Wu and J. Zhang, *Adv. Synth. Catal.*, 2018, **360**, 2144–2150.
94 T. Mino, Y. Sato, A. Saito, Y. Tanaka, H. Saotome, M. Sakamoto and T. Fujita, *J. Org. Chem.*, 2005, **70**, 7979–7984.
95 C. Bonaccorsi, S. Bachmann and A. Mezzetti, *Tetrahedron: Asymmetry*, 2003, **14**, 845–854.
96 P. E. Sues, A. J. Lough and R. H. Morris, *Organometallics*, 2011, **30**, 4418–4431.
97 C.-J. Wang, F. Gao and G. Liang, *Org. Lett.*, 2008, **10**, 4711–4714.
98 (*a*) C.-J. Wang, G. Liang, Z.-Y. Xue and F. Gao, *J. Am. Chem. Soc.*, 2008, **130**, 17250–17251; (*b*) Q.-H. Li, M.-C. Tong, J. Li,

H.-Y. Taoa and C.-J. Wang, *Chem. Commun.*, 2011, **47**, 11110–11112; (*c*) T.-L. Liu, Z.-L. He, H.-Y. Tao, Y.-P. Cai and C.-J. Wang, *Chem. Commun.*, 2011, **47**, 2616–2618; (*d*) Q.-H. Li, L. Wei, X. Chen and C.-J. Wang, *Chem. Commun.*, 2013, **49**, 6277–6279; (*e*) J. Li, H.-Y. Tao and C.-J. Wang, *Chem. Commun.*, 2017, **53**, 1657–1659.

99 (*a*) C.-J. Wang, Z.-Y. Xue, G. Liang and Z. Lu, *Chem. Commun.*, 2009, 2905–2907; (*b*) G. Liang, M.-C. Tong and C.-J. Wang, *Adv. Synth. Catal.*, 2009, **351**, 3101–3106; (*c*) Z.-Y. Xue, T.-L. Liu, Z. Lu, H. Huang, H.-Y. Tao and C.-J. Wang, *Chem. Commun.*, 2010, **46**, 1727–1729.

100 P. H. S. Paioti, K. A. Abboud and A. Aponick, *ACS Catal.*, 2017, **7**, 2133–2138.

101 (*a*) F. S. P. Cardoso, K. A. Abboud and A. Aponick, *J. Am. Chem. Soc.*, 2013, **135**, 14548–14551; (*b*) S. Mishra, J. Liu and A. Aponick, *J. Am. Chem. Soc.*, 2017, **139**, 3352–3355.

102 X. Hu, C. Bai, H. Dai, H. Chen and Z. Zheng, *J. Mol. Catal. A: Chem.*, 2004, **218**, 107–112.

103 X. Li, X. Jia, L. Xu, S. H. L. Kok, C. W. Yip and A. S. C. Chan, *Adv. Synth. Catal.*, 2005, **347**, 1904–1908.

104 X.-X. Yan, Q. Peng, Y. Zhang, K. Zhang, W. Hong, X.-L. Hou and Y.-D. Wu, *Angew. Chem. Int. Ed.*, 2006, **45**, 1979–1983.

105 Z.-W. Lai, R.-F. Yang, K.-Y. Ye, H. S. Sun and S.-L. You, *Beilstein J. Org. Chem.*, 2014, **10**, 1261–1266.

106 (*a*) X. Bai, C. Wu, S. Ge and Y. Lu, *Angew. Chem. Int. Ed.*, 2020, **59**, 2764–2768; (*b*) D. J. Cowan, J. L. Collins, M. B. Mitchell, J. A. Ray, P. W. Sutton, A. A. Sarjeant and E. E. Boros, *J. Org. Chem.*, 2013, **78**, 12726–12734.

107 (*a*) F. Brüning, H. Nagae, D. Käch, K. Mashima and A. Togni, *Chem.–Eur. J.*, 2019, **25**, 10818–10822; (*b*) X. Feng, B. Pugin, E. Kusters, G. Sedelmeier and H.-U. Blaser, *Adv. Synth. Catal.*, 2007, **349**, 1803–1807.

108 (*a*) Q. Zhao, S. Li, K. Huang, R. Wang and X. Zhang, *Org. Lett.*, 2013, **15**, 4014–4017; (*b*) Q. Zhao, J. Wen, R. Tan, K. Huang, P. Metola, R. Wang, E. V. Anslyn and X. Zhang, *Angew. Chem. Int. Ed.*, 2014, **126**, 8607–8610; (*c*) J. Wen, R. Tan, S. Liu, Q. Zhao and X. Zhang, *Chem. Sci.*, 2016, **7**, 3047–3051.

109 (*a*) T. Sturm, W. Weissensteiner and F. Spindler, *Adv. Synth. Catal.*, 2003, **345**, 160–164; (*b*) Y. Wang, T. Sturm, M. Steurer, V. B. Arion, K. Mereiter, F. Spindler and W. Weissensteiner, *Organometallics*, 2008, **27**, 1119–1127; (*c*) A. Saito, N. Kumagai and M. Shibasaki, *Angew. Chem. Int. Ed.*, 2017, **56**, 5551–5555.

110 (*a*) T. M. Konrad, J. T. Durrani, C. J. Cobley and M. L. Clarke, *Chem. Commun.*, 2013, **49**, 3306–3308; (*b*) S. H. Gilbert, S. Tin, J. A. Fuentes, T. Fanjul and M. L. Clarke, *Tetrahedron*, 2021, **80**, 131863.

111 L. Leseurre, F. Le Boucher d'Herouville, K. Püntener, M. Scalone, J.-P. Genêt and V. Michelet, *Org. Lett.*, 2011, **13**, 3250–3253.

112 (*a*) T. Korenaga, K. Osaki, R. Maenishi and T. Sakai, *Org. Lett.*, 2009, **11**, 2325–2328; (*b*) T. Korenaga, R. Maenishi, K. Hayashi and T. Sakai, *Adv. Synth. Catal.*, 2010, **352**, 3247–3254.

113 J. H. Koh, A. O. Larsen and M. R. Gagné, *Org. Lett.*, 2001, **3**, 1233–1236.

114 F. Le Boucher d'Herouville, A. Millet, M. Scalone and V. Michelet, *J. Org. Chem.*, 2011, **76**, 6925–6930.

115 M. Scalone and P. Waldmeier, *Org. Process Res. Dev.*, 2003, **7**, 418–425.

116 K. Aikawa, K. Yabuuchi, K. Torii and K. Mikami, *Beilstein J. Org. Chem.*, 2018, **14**, 576–582.

117 B. Drießen-Höscher, J. Kralik, F. Agel, C. Steffens and C. Hu, *Adv. Synth. Catal.*, 2004, **346**, 979–982.

118 (*a*) D.-Y. Zhang, C.-B. Yu, M.-C. Wang, K. Gao and Y.-G. Zhou, *Tetrahedron Lett.*, 2012, **53**, 2556–2559; (*b*) D.-Y. Zhang, D.-S. Wang, M.-C. Wang, C.-B. Yu, K. Gao and Y.-G. Zhou, *Synthesis*, 2011, 2796–2802.

119 (*a*) S. Jeulin, S. Duprat de Paule, V. Ratovelomanana-Vidal, J.-P. Genêt, N. Champion and P. Dellis, *Angew. Chem. Int. Ed.*, 2004, **43**, 320–325; (*b*) D. E. Kim, C. Choi, I. S. Kim, S. Jeulin, V. Ratovelomanana-Vidal, J.-P. Genêt and N. Jeong, *Adv. Synth. Catal.*, 2007, **349**, 1999–2006; (*c*) Z. Yan, B. Wu, X. Gao, M.-W. Chen and Y.-G. Zhou, *Org. Lett.*, 2016, **18**, 692–695; (*d*) L. Yin, L. Brewitz, N. Kumagai and M. Shibasaki, *J. Am. Chem. Soc.*, 2014, **136**, 17958–17961.

120 F. Berhal, O. Esseiva, C.-H. Martin, H. Tone, J.-P. Genet, T. Ayad and V. Ratovelomanana-Vidal, *Org. Lett.*, 2011, **13**, 2806–2809.

121 (*a*) H.-P. Xie, Z. Yan, B. Wu, S.-B. Hu and Y.-G. Zhou, *Tetrahedron Lett.*, 2018, **59**, 2960–2964; (*b*) S.-B. Hu, Z.-P. Chen, J. Zhou and Y.-G. Zhou, *Tetrahedron Lett.*, 2016, **57**, 1925–1929.

122 M. Murata, T. Morimoto and K. Achiwa, *Synlett*, 1991, 827–828.

123 (*a*) N. Armanino, R. Koller and A. Togni, *Organometallics*, 2010, **29**, 1771–1777; (*b*) D. E. Kim, C. Choi, I. S. Kim, S. Jeulin, V. Ratovelomanana-Vidal, J.-P. Genêt and N. Jeong, *Synthesis*, 2006, 4053–4059; (*c*) N. Jeong, D. H. Kim and J. H. Choi, *Chem. Commun.*, 2004, 1134–1135.

124 Y. Nakamura, S. Takeuchi, S. Zhang, K. Okumura and Y. Ohgo, *Tetrahedron Lett.*, 2002, **43**, 3053–3056.

125 (*a*) J. Horn and W. Bannwarth, *Eur. J. Org. Chem.*, 2007, 2058–2063; (*b*) V. Andrushko, D. Schwinn, C. C. Tzschucke, F. Michalek, J. Horn, C. Mössner and W. Bannwarth, *Helv. Chim. Acta*, 2005, **88**, 936–949.

126 (*a*) E. G. Hope, A. M. Stuart and A. J. West, *Green Chem.*, 2004, **6**, 345–350; (*b*) D. J. Birdsall, E. G. Hope, A. M. Stuart, W. Chen, Y. Hu and J. Xiao, *Tetrahedron Lett.*, 2001, **42**, 8551–8553.

127 J. Bayardon, M. Cavazzini, D. Maillard, G. Pozzi, S. Quici and D. Sinou, *Tetrahedron: Asymmetry*, 2003, **14**, 2215–2224.

128 (*a*) G. Franciò, K. Wittmann and W. Leitner, *J. Organomet. Chem.*, 2001, **621**, 130–142; (*b*) G. Franciò and W. Leitner, *Chem. Commun.*, 1999, 1663–1664.

129 D. Bonafoux, Z. Hua, B. Wang and I. Ojima, *J. Fluorine Chem.*, 2001, **112**, 101–108.

130 (*a*) L. Wang, W. Meng, C.-L. Zhu, Y. Zheng, J. Nie and J.-A. Ma, *Angew. Chem. Int. Ed.*, 2011, **50**, 9442–9446; (*b*) P.-S. Wang, P. Liu, Y.-J. Zhai, H.-C. Lin, Z.-Y. Han and L.-Z. Gong, *J. Am. Chem. Soc.*, 2015, **137**, 12732–12735; (*c*)

P.-S. Wang, M.-L. Shen, T.-C. Wang, H.-C. Lin and L.-Z. Gong, *Angew. Chem. Int. Ed.*, 2017, **56**, 16032–16036; (*d*) H.-C. Lin, P.-S. Wang, Z.-L. Tao, Y.-G. Chen, Z.-Y. Han and L.-Z. Gong, *J. Am. Chem. Soc.*, 2016, **138**, 14354–14361.

131 F.-N. Sun, W.-C. Yang, X.-B. Chen, Y.-L. Sun, J. Cao, Z. Xu and L.-W. Xu, *Chem. Sci.*, 2019, **10**, 7579–7583.

132 M. V. Escárcega-Bobadilla, L. Rodríguez-Pérez, E. Teuma, P. Serp, A. M. Masdeu-Bultó and M. Gómez, *Catal. Lett.*, 2011, **141**, 808–816.

133 (*a*) T. Yamamoto, Y. Akai, Y.-U. Nagata and M. Suginome, *Angew. Chem. Int. Ed.*, 2011, **50**, 8844–8847; (*b*) H. Yamamoto and M. Suginome, *Angew. Chem. Int. Ed.*, 2009, **48**, 539–542.

134 A. Klose and J. A. Gladysz, *Tetrahedron: Asymmetry*, 1999, **10**, 2665–2674.

135 U. Nettekoven, M. Widhalm, H. Kalchhauser, P. C. J. Kamer, P. W. N. M. van Leeuwen, M. Lutz and A. L. Spek, *J. Org. Chem.*, 2001, **66**, 759–770.

136 B. J. Anderson, D. S. Glueck, A. G. DiPasquale and A. L. Rheingold, *Organometallics*, 2008, **27**, 4992–5001.

137 T. V. RajanBabu, T. A. Ayers, G. A. Halliday, K. K. You and J. C. Calabrese, *J. Org. Chem.*, 1997, **62**, 6012–6028.

138 L. B. Fields and E. N. Jacobsen, *Tetrahedron: Asymmetry*, 1993, **4**, 2229–2240.

139 M. Cavazzini, G. Pozzi, S. Quici, D. Maillard and D. Sinou, *Chem. Commun.*, 2001, 1220–1221.

140 S. Handa and L. M. Slaughter, *Angew. Chem. Int. Ed.*, 2012, **51**, 2912–2915.

141 K. B. Selim, H. Nakanishi, Y. Matsumoto, Y. Yamamoto, K.-i. Yamada and K. Tomioka, *J. Org. Chem.*, 2011, **76**, 1398–1408.

142 (*a*) A. M. Sorlin, J. C. Mixdorf, M. E. Rotella, R. T. Martin, O. Gutierrez and H. M. Nguyen, *J. Am. Chem. Soc.*, 2019, **141**, 14843–14852; (*b*) J. C. Mixdorf, A. M. Sorlin, Q. Zhang and H. M. Nguyen, *ACS Catal.*, 2018, **8**, 790–801; (*c*) Q. Zhang, D. P. Stockdale, J. C. Mixdorf, J. J. Topczewski and H. M. Nguyen, *J. Am. Chem. Soc.*, 2015, **137**, 11912–11915.

143 (*a*) R. Takeshi and T. Nishimura, *Org. Biomol. Chem.*, 2015, **13**, 4918–4924; (*b*) T. Nishimura, H. Kumamoto, M. Nagaosa and T. Hayashi, *Chem. Commun.*, 2009, 5713–5715.

144 (*a*) T. Nishimura, J. Wang, M. Nagaosa, K. Okamoto, R. Shintani, F.-y. Kwong, W.-y. Yu, A. S. C. Chan and T. Hayashi, *J. Am. Chem. Soc.*, 2010, **132**, 464–465; (*b*) T. Nishimura, M. Nagaosa and T. Hayashi, *Chem. Lett.*, 2008, **37**, 860–861; (*c*) T. Nishimura, Y. Yasuhara, T. Sawano and T. Hayashi, *J. Am. Chem. Soc.*, 2010, **132**, 7872–7873.

145 (*a*) M. Nagamoto, T. Yanagi, T. Nishimura and H. Yorimitsu, *Org. Lett.*, 2016, **18**, 4474–4477; (*b*) T. Nishimura, Y. Yasuhara, M. Nagaosa and T. Hayashi, *Tetrahedron: Asymmetry*, 2008, **19**, 1778–1783.

146 T. Nishimura, Y. Ichikawa, T. Hayashi, N. Onishi, M. Shiotsuki and T. Masuda, *Organometallics*, 2009, **28**, 4890–4893.